Polymer Journal, Vol. 39, No. 9, pp. 889–922 (2007)

AWARD ACCOUNTS: SPSJ WILLY AWARD (2006)

Dendritic Architectures for Design of Photo– and Spin–Functional Nanomaterials

Zheng HE,[1] Tomoya ISHIZUKA,[1] and Donglin JIANG[1,2,†]

[1]*Department of Materials Molecular Science, Institute for Molecular Science, National Institutes of Natural Sciences, 5-1 Higashiyama, Myodaiji, Okazaki 444-8787, Japan*
[2]*Precursory Research for Embryonic Science and Technology, Japan Science and Technology Agency, 5-1 Higashiyama, Myodaiji, Okazaki 444-8787, Japan*

(Received April 6, 2007; Accepted April 24, 2007; Published June 12, 2007)

ABSTRACT: Unlike ordinary linear polymers, dendritic architecture is unique in the terms of its elaborative capability for total control over molecular design parameters at the single molecular level, *i.e.*, molecular size, branching pattern, structure, and morphology, thereby provides a new platform for the creation of functional materials with nanometer–scale precision. This review mainly concerns recent works on the development of dendritic nanomaterials with a focus on photo– and spin–related functionalities. Strategy for the incorporation of chromophores to build up light–harvesting antennae is presented with an emphasis on morphology and size effects. Dendritic macromolecules for photoinduced electron transfer are categorized based on chromophores that serve as the active center to absorb light and trigger photochemical process. In this context, dendrimers bearing porphyrin, conjugated polymer, and fullerene for realization of long–lived charge–separation state and light energy conversion are highlighted. On the other hand, design of dendritic macromolecules for spin–functional materials is focused on dendronized organic radicals and dendritic coordination polymers. Especially, spin–functional soft materials with an aim for spin manipulation and novel magnetic–optical switches are emphasized. [doi:10.1295/polymj.PJ2007006]

KEY WORDS Dendrimer / Light Harvesting / Photoinduced Energy Transfer / Photoinduced Electron Transfer / Magnetic Soft Materials / Spin Transition / Radicals /

Dendritic architecture, characterized by its iteratively branched structure, is one of the most pervasive topology, which can be easily found at a variety of dimensional scales such as in abiotic phenomena including snow crystals and lightning patterns, and in biological systems, for example, tree branches and neuron networks. From a synthetic point of view, such architecture will enable chemists to construct molecules with their components linked in a radial fashion, which is hardly achieved *via* ordinary synthetic methodology. With the development of two main strategies, *i.e.* divergent and convergent approaches,[1–3] innumerable dendritic structures have been reported up to date. 'Dendrimer' termed by Tomalia in 1985 has been recognized as the fourth major class of macromolecular architectures. Benefiting from the well–established synthetic strategies, chemists are now able to precisely control the size and shape of the dendrimer frameworks as well as the numbers and positions of the functional groups. This molecular design flexibility is one of the most unique characters, which distinguished dendrimers from all other linear, hyperbranched, and star–shaped macromolecules.

On the other hand, the myriad of sophisticated natural processes such as light harvesting, energy transduction and conversion stimulated chemists in the design of various functional molecules and their assemblies, which lead to many significant scientific and technological advances over the past decades. In relation to this, dendritic architecture, due to its well–defined morphology, provides a new platform for exploring novel materials with nanometer scale precision. Recent studies on dendrimers have extended the scope of research from synthesis to applications for catalysts, photoactive and electronic materials, medicinal and biomedical materials, and other functional materials.[4,5] In this review, we focused on recent works on functional dendrimers, for light-harvesting and photoinduced energy transduction, for photoinduced electron transfer to achieve long–term charge–separation state and trigger hydrogen evolution from water, for controlled self-assembly to fabricate photofunctional nanomaterials with well–defined structure, and for spin manipulation to control spin state of dendritic radicals and polynuclear metal chains, with an emphasis on correlation between structures and properties of these dendritic macromolecules.

[†]To whom correspondence should be addressed (Tel: +81-564-59-5520, Fax: +81-564-59-5520, E-mail: jiang@ims.ac.jp).

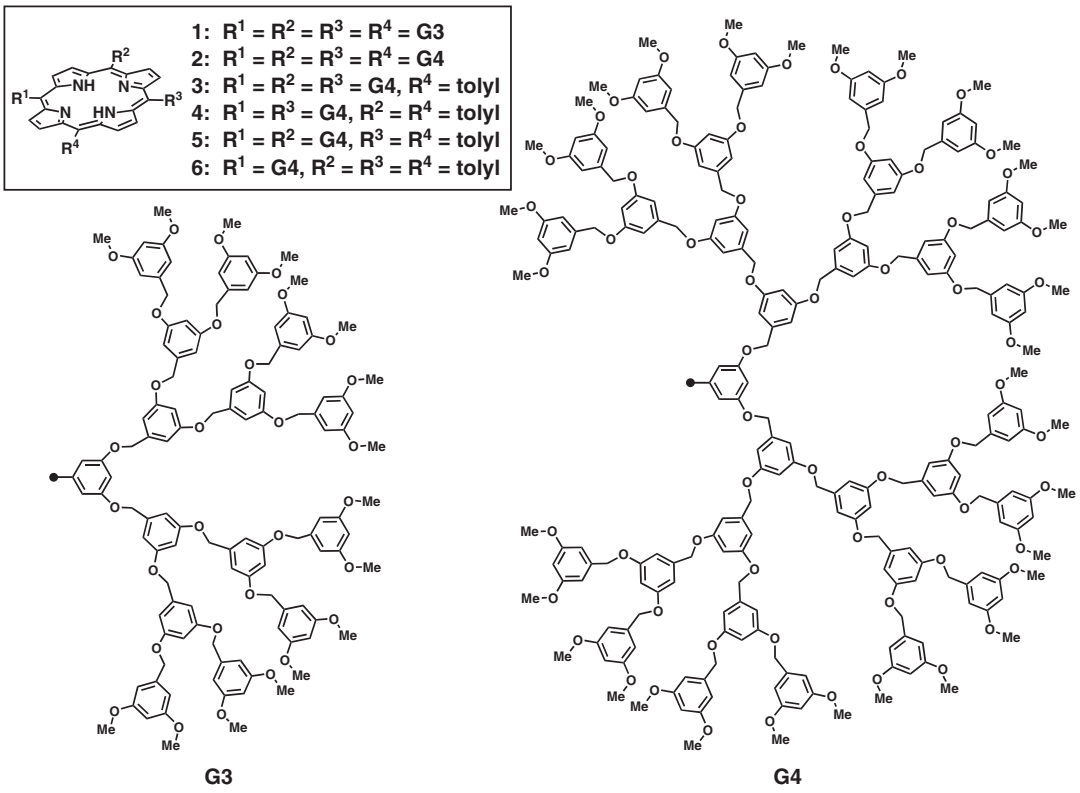

DENDRITIC ARCHITECTURES FOR PHOTOINDUCED ENERGY TRANSFER

Photosynthesis that transforms carbon dioxide and water to glucose and oxygen discovered in plants and photosynthetic bacteria, is triggered by a highly efficient photoinduced energy transfer from light–harvesting antennae to photosynthetic reaction center, where photoinduced electron transfer takes place to initiate the conversion of solar energy into chemical energy.[6,7] To trap low–density solar photons, natural photosynthetic systems have developed multi–chlorophyll based wheel–like arrays, which enable ultrafast intra– and inter–wheel energy transfer and channel excitation energy to special pair at 100% quantum yield.[8] Such an elaborate energy transduction system inspired chemists to develop artificial light–harvesting antenna systems, with an aim for realizing efficient and vectorial photoinduced energy transfer.

Due to their capability for accommodating a large number of chromophores in their nano–sized frameworks together with a well–defined three–dimensional structure, dendrimers are attractive motif for creation of artificial light–harvesting antennae. Up to date, a variety of photofunctional dendrimers have been synthesized upon incorporating chromophore units at the focal core, in the interior blocks, and on the exterior surface. From a viewpoint of molecular design, mainly two approaches have been developed to utilize dendritic architecture for constructing artificial light–harvesting antennae. One way is to employ chromophore units as building blocks for a dendrimer and thereby the whole framework serves as an antenna. An alternative strategy is to anchor dye units on the exterior surface of the dendrimer framework. In this case, the dendrimer framework functions as a scaffold to connect the exterior donor moieties with a focal acceptor unit and intervenes the intramolecular energy transfer event. So far, both convergent and divergent methodologies have been applied for site–specific placement of dye components for the construction of light–harvesting antennae.

Antennae for Ultraviolet Light Harvesting

Poly(benzyl ether) dendrimers with porphyrin functionality have been synthesized by convergent method *via* coupling reactions of dendron subunits with a porphyrin core.[9,10] Owing to the fact that *meso*–phenyl groups are nearly perpendicular to the porphyrin plane, the fully substituted dendrimer porphyrins **1** and **2** adopt a spherical three–dimensional morphology, whereas those partially–substituted homologues (**3**–**6**) resemble a corn–like structure. Upon excitation at 280 nm, which is an absorption band due to the poly(benzyl ether) dendrimer framework, **1** and **2** emit mainly a fluorescence from the porphyrin core at 656 and 718 nm. Since the dendrimer framework itself emits at 310 nm, the emission from porphyrin core observed for **1** and **2** is clearly the result of an intramo-

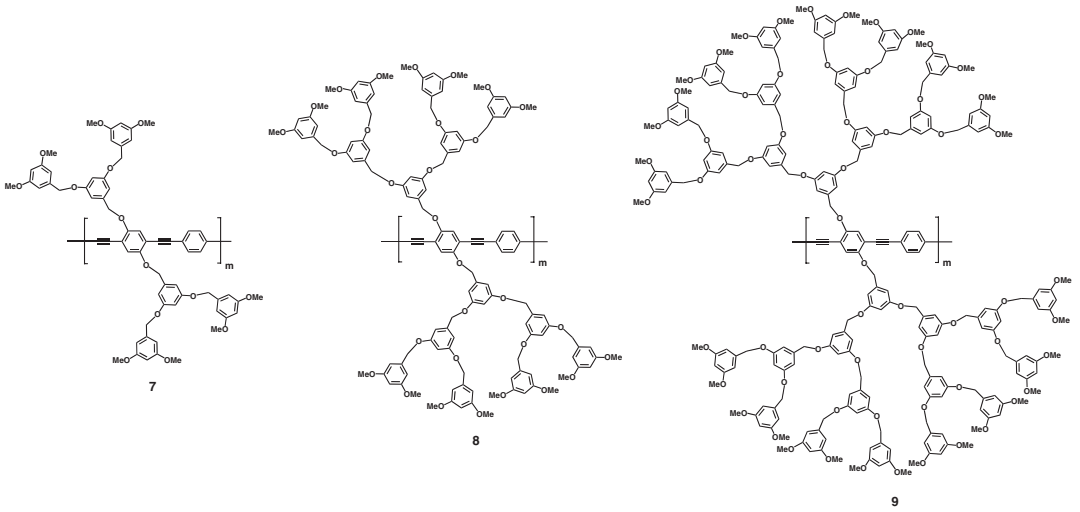

lecular energy transfer from the dendrimer framework to the focal porphyrin unit. In comparison with excitation fluorescence spectrum, the efficiency of energy transfer of **1** and **2** has been evaluated to be 80%. In sharp contrast, partially substituted **3**, although bearing three large dendron subunits in its framework, exhibits a quite low energy transfer efficiency to be only 30%. This decreasing tendency in energy transfer efficiency is more explicit when the number of the dendritic wedges becomes less, where one–dendron substituted **6** shows an efficiency as low as 10%. These results demonstrate that the intramolecular energy transfer event is highly dependent on the morphology of the dendritic macromolecules.

Fluorescence anisotropy measurements reveal that excitation energy is not localized but is able to migrate efficiently over the continuous dendrimeric array of the chromophoric building units surrounding the energy trap. Consequently, for the spherical dendrimer, the probability of energy transfer to the porphyrin core is greatly enhanced. On the other hand, non–spherical dendrimers have a much looser and discontinuous dendrimeric array of the aromatic units, where the energy migration should be less efficient. As the result, the most excitation energy is lost by radiation before transferred to the energy trap. This finding is interesting with respect to the energy transduction events observed for the wheel–like arrays of chromophores in natural photosynthetic system, where the efficient cooperation of chromophores allows rapid excitation energy migration along the wheels, followed by transfer to the focal special pair to initiate the photosynthesis. In this sense, this work offers a new strategy for the molecular design of light–harvesting materials.

In relation to above results, poly(benzyl ether) dendron, capable of UV light harvesting, has been attached to conjugated polymer chains to afford dendritic polymeric wires.[11–14] Due to their conformational rigidity, conjugated polymers have limited solubility and are difficult to process. On the other hand, from a photochemical point of view, their high tendency to form aggregates also leads to collisional energy dissipation and eventually spoils their utility as light emitter. When a conjugate poly(phenyleneethynylene) backbone is appended with flexible poly(benzyl ether) dendritic wedges, the resultant rod–like dendritic conjugated polymers (**7**–**9**) become highly soluble in common organic solvents such as THF, benzene, dichloromethane, and chloroform. In addition, simple casting of the polymer solutions gives a homogenous thin film. Upon direct excitation of the polymer backbone in THF, dendrimer rod **9** bearing the largest dendritic envelope emits a strong blue fluorescence centered at 454 nm with the quantum yield (Φ_{FL}) around 100%, which remains constant over a wide range of concentration. However, **7** and **8** with smaller dendritic wedges exhibit a significant concentration–dependent fluorescence activity. Although **8** shows a high Φ_{FL} value around 100% in dilute solution ($Abs_{431\,nm} = 0.01$), this value drops to 67% when the solution is concentrated to give $Abs_{431\,nm}$ of 0.1. This phenomenon is much explicit for the lowest–generation **7**, whose Φ_{FL} value is only 56% in dilute condition and further decreases upon concentration. The large dendrimeric framework is likely to encapsulate the conjugated backbone as an envelope and prevents the photoexcited state from collisional quenching. Such a dendrimer size–dependent luminescence activity of conjugated backbone has been observed again for dendritic conjugated polymers with discrete lengths.[15]

The intramolecular singlet energy transfer from the dendrimer framework to the focal conjugated backbone has been investigated upon excitation of the dendritic wedge at 278 nm by the use of fluorescence spectroscopy. As a result, all these dendritic rods emit blue light without any luminescence from the dendrit-

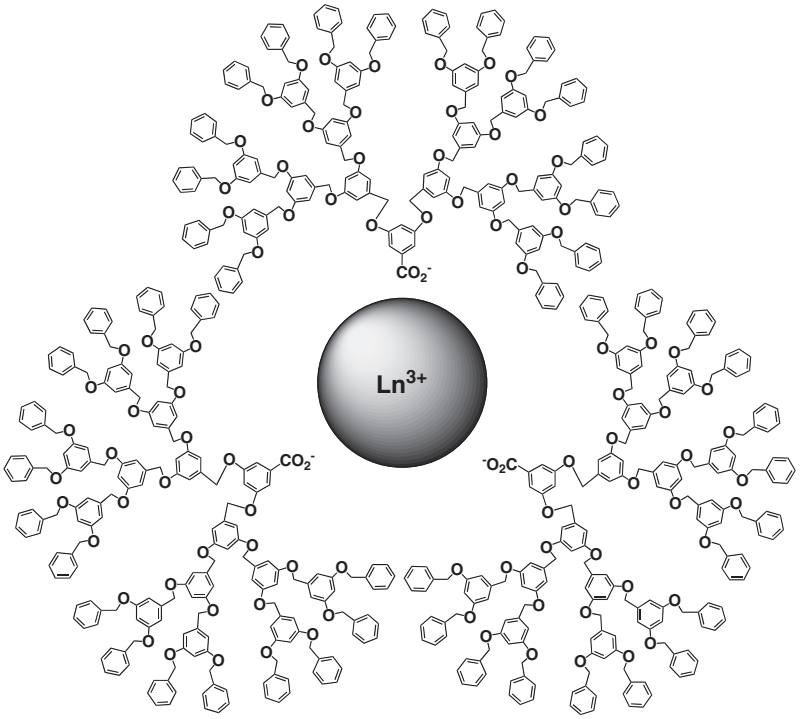

10

ic wedges, where the energy transfer efficiency value has been evaluated to be 100%. Owing to the prominent light–harvesting function together with efficient site–isolation effect of the large dendritic envelope, the luminescence activity of the conjugated backbone is significantly enhanced. Notably, the luminescence of **9** upon excitation of dendritic wedges is 12 folds more intense than that of **7** under identical conditions. Therefore, dendritic conjugated polymer **9** with a large dendrimer framework severs as an excellent organic light emitter, which can efficiently collect photons of a rather wide wavelength range from ultraviolet to visible, and convert them to blue luminescence at a quantum yield near 100%.

Artificial light–harvesting antennae coupled with lanthanide complexes, owing to their potential photonic utility as optical signal amplifiers, light–emitting diodes, and luminescent probes, have attracted much attention in recent years. Compared with other emitters, lanthanide complexes are characterized by a relatively long lifetime of the excitation state along with a narrow emission band.[16] However, the excitation energy of lanthanide complex is easily dissipated through collision with solvent molecules and/or vibrational escape to neighboring units with high vibrational modes. For these reasons, one important issue in designing luminescent lanthanide complex is to spatially isolate lanthanide center from environment. By taking advantages of the coordination chemistry of carboxylic acid with lanthanide metal ions, Kawa and coworkers have used poly(benzyl ether) ligand bearing benzoic acid unit at the focal core, for self–assembly with lanthanide ions such as Eu^{3+}, Tb^{3+}, and Er^{3+}, to synthesize dendritic lanthanide complex (**10**).[17–19] Excitation on the dendrimer framework at 280 nm induces predominant luminescence from the focal Tb^{3+} and Eu^{3+} ions at 545 and 615 nm, respectively, indicating intramolecular energy transfer to the focal lanthanide core. As a result of suppressed self–quenching upon encapsulation within the large dendrimer framework, the luminescence efficiency is greatly enhanced with the generation number. To clarify site–isolation effect of dendritic wedges, Kim and coworkers have employed poly(benzyl ether) dendrons bearing a focal anthracene carboxylic acid unit to coordinate with Ln^{3+} in the presence of terpyridine as a co–ligand.[20] A film of Er^{3+} complex **11**, upon excitation of the anthracene unit at 357 nm, emits at 1530 nm, whose intensity is 4.8 times stronger than that upon excitation of poly(benzyl ether) dendron at 290 nm. As the generation number of the dendrons increases from 0 to 3, the emission intensity is enhanced by more than 100 folds upon excitation at the anthracene unit. This demonstrates an efficient site–isolation of the Er^{3+} core with the large poly(benzyl ether) dendrons that prevents its excitation state from collisional self–quenching.

In addition to the carboxylic unit as a coordination group, amide groups have been utilized for the synthesis of lanthanide–dendrimer complexes. Polylysin dendrimer **12** with 24 dansyl groups as light-absorbing units on the exterior surface and 21 amide units in the

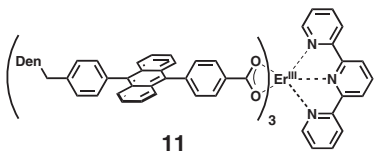

11

Den =

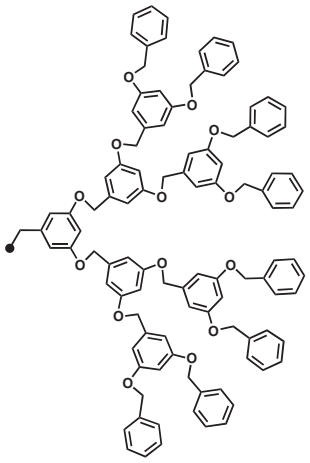

G3

interior, has been found to host Ln^{3+} ions.[21,22] Upon excitation of the dansyl groups at 343 nm, **12** itself emits at 514 nm with a Φ_{FL} value of 28%. Addition of Ln^{3+} to **12** results in a significant quenching of fluorescence at 514 nm, along with a new emission band of Ln^{3+} in the near–IR region, suggesting that the excitation energy absorbed by the dansyl units can be channeled to the focal Ln^{3+} core.

Laser dyes are attractive motifs for the construction of light–harvesting antennae due to their large absorption cross–section and high luminescence efficiency. Fréchet and coworkers have developed a series of laser dye–labeled dendrimers. Coumarin 2 has been selected as the donor to anchor on the surface of poly(benzyl ether) dendrons **13–16** containing a focal Coumarin 343 unit as an energy trap.[23,24] In this case, poly(benzyl ether) dendrimer framework is photochemically silent, serving as a scaffold to link donor and acceptor units and mediating the energy transfer process. **13–16** exhibit an efficient energy transfer from Coumarin 2 units on the exterior surface to the focal Coumarin 343 core, as evidenced by a strong emission band at 470 nm from Coumarin 343 upon excitation of Coumarin 2 moieties. The energy transfer through the poly(benzyl ether) framework is dominated by Förster–type mechanism and this event is extremely fast with a rate constant higher than $3.3 \times 10^{-10}\ s^{-1}$. Considering the fact that the energy transfer efficiency of **13–16** is similar to one another, their light–harvesting activity is in proportion with the number of Coumarin 2 units on the exterior surface of the dendrimer framework.

In general, Förster–type energy transfer is highly dependent on the spectral overlap and transition dipole moment.[25] This is the same case for the intramolecular energy transfer observed for **16**. A comparison study has been carried out on compounds **17** and **18** with oligothiophene as the focal energy trap in place of Coumarin 343.[26] As oligothiophene has a larger spectral overlap with Coumarin 2 and a higher transi-

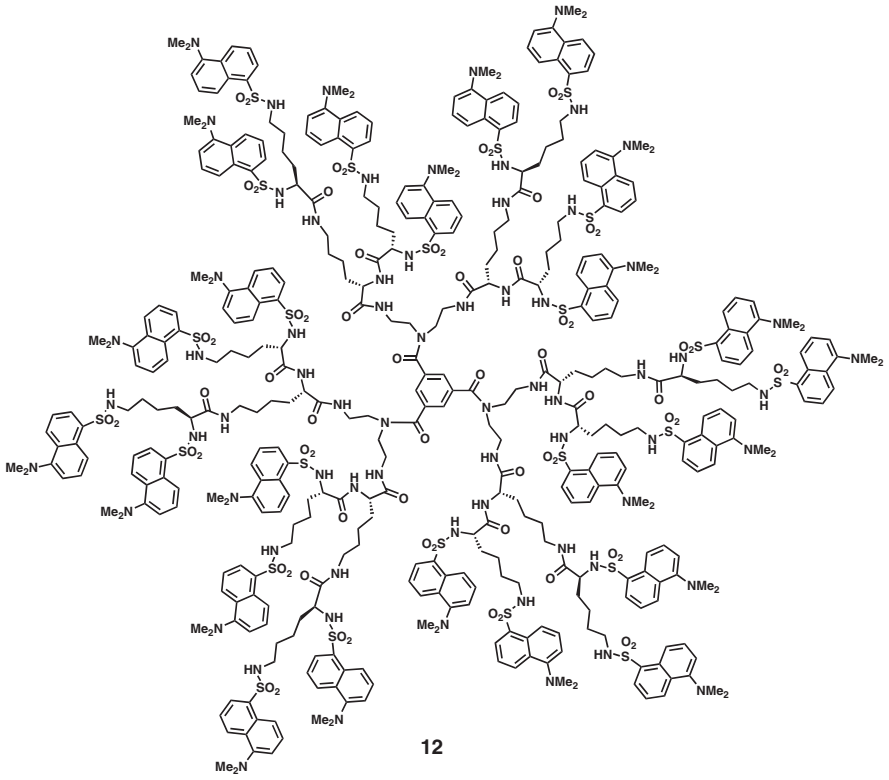

12

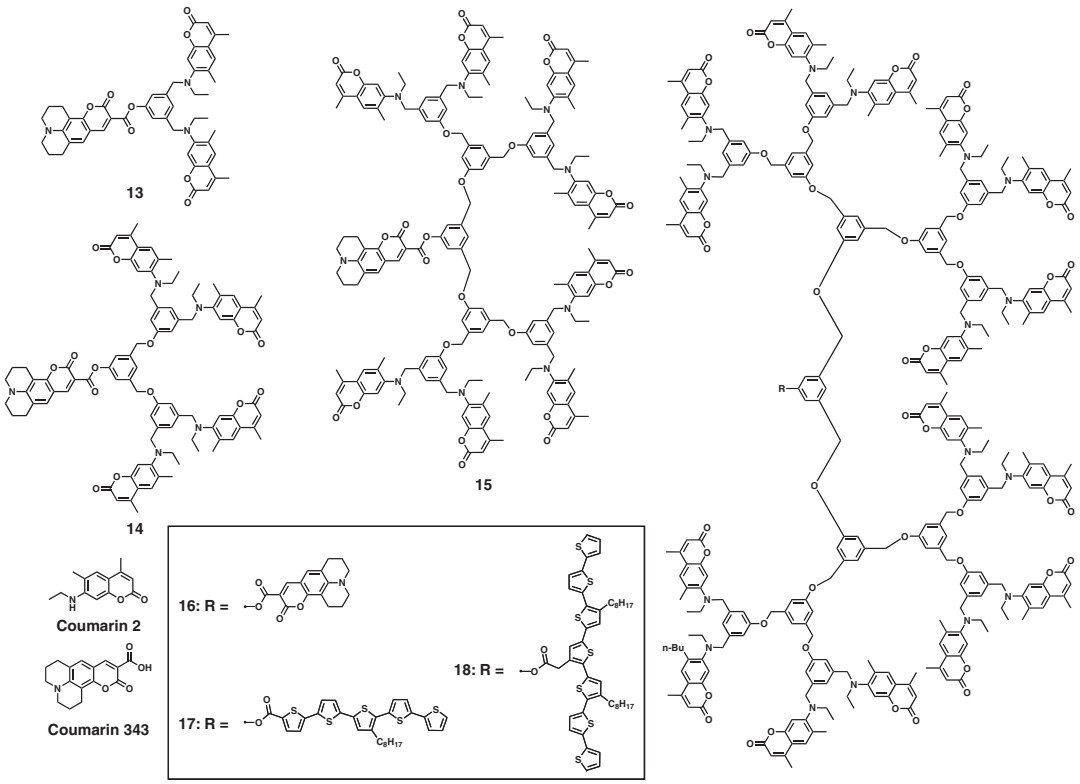

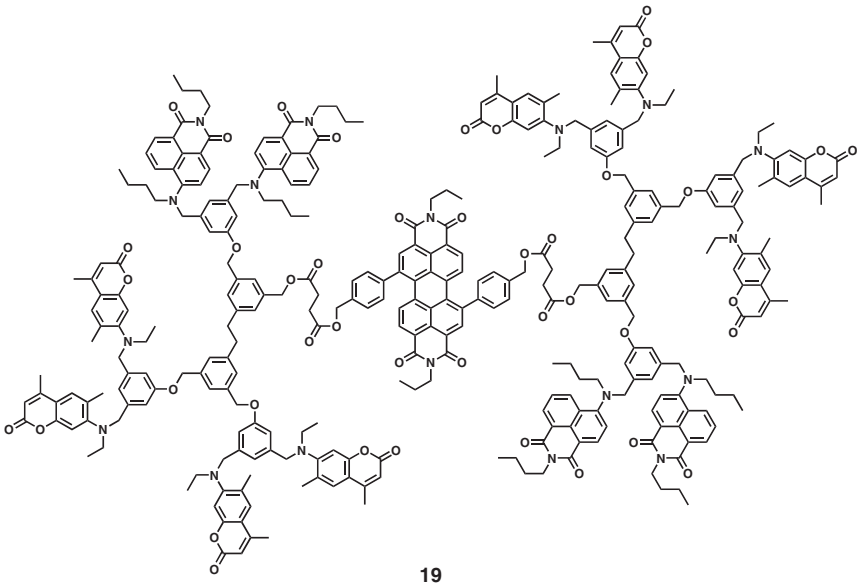

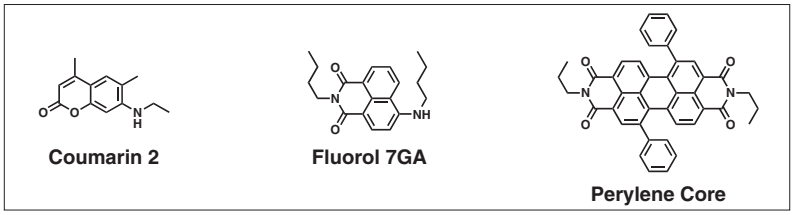

tion dipole moment than those of Coumarin 343, the efficiency of energy transfer from Coumarin 2 to the oligothiophene unit is nearly 100%. On the basis of the above results, three different chromophores, *i.e.* Coumarin 2 and fluorol 7GA moieties as donors in the outer layers and the perylene unit as an acceptor at the focal core, have been incorporated for the synthesis of a dendritic triad **19**.[27] Because there is no

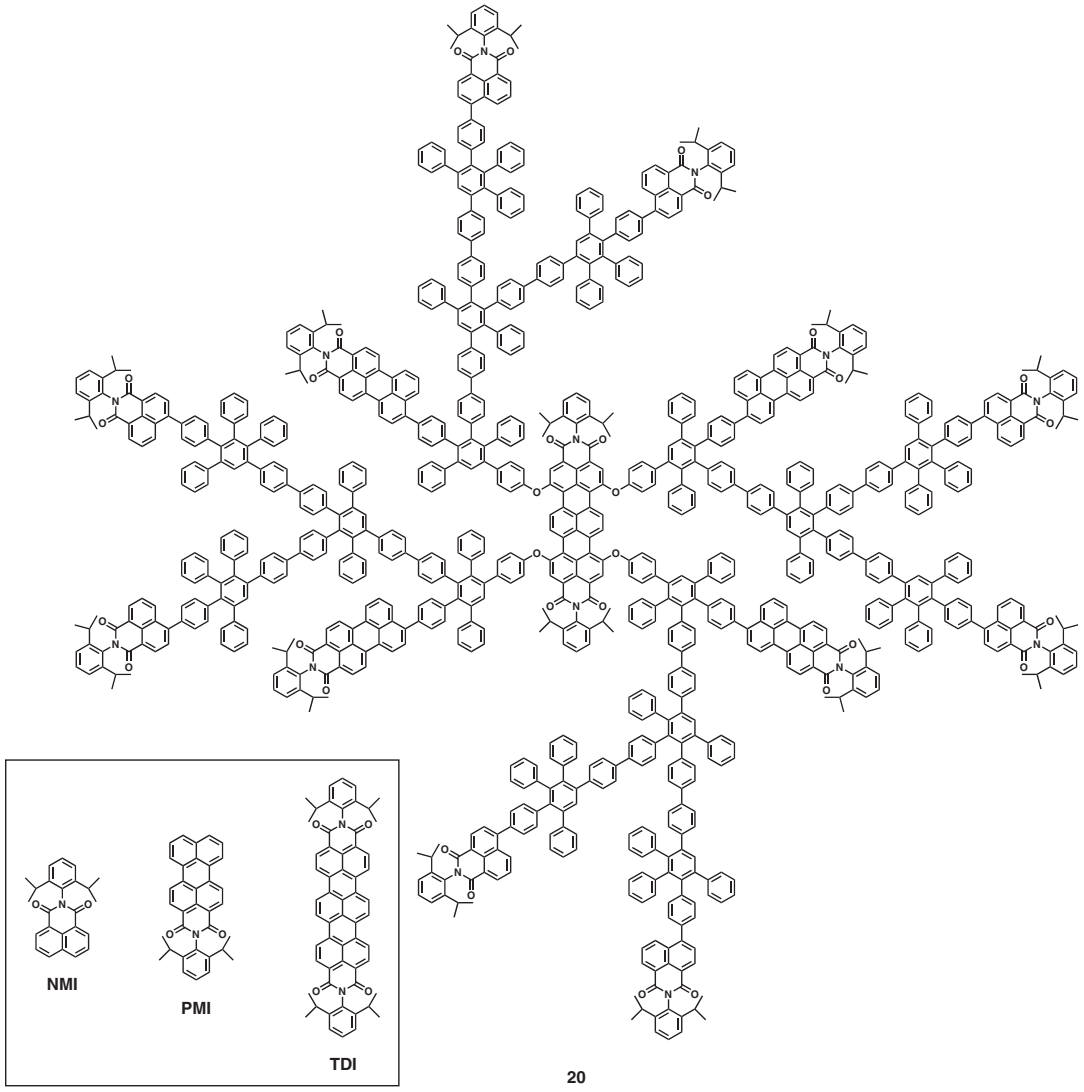

20

spectral overlap between Coumarin 2 and the perylene units, it is expected that the energy transfer in **19**, if any occurs upon excitation of Coumarin 2 unit, should be in a cascade way involving the mediation of fluorol 7GA. Indeed, excitation of the Coumarin 2 unit at 342 nm gives an emission at 610 nm due to the focal perylene unit with intensity 6.9 folds that of direct excitation at 555 nm. This indicates that the excitation energy of the Coumarin 2 on the dendrimer surface can be funneled to the focal perylene trap through a vectorial two–step process mediated by fluorol 7GA. The overall energy transfer efficiency from the exterior Coumarin 2 moiety to the focal perylene unit is higher than 95%, and each step with an efficiency of 98%.

In contrast to conformationally flexible dendrimer frameworks, rigid scaffolds, *c.f.* polyphenylene dendrimer has been utilized for the construction of light–harvesting antenna.[28] Weil, Müllen, and coworkers have reported a stepwise energy transfer process in a shape–persistent polyphenylene dendrimer **20** that bears three layered chromophores, with terrylene tetracarboxydiimide (TDI) as acceptor, perylene dicarboxymonoimide (PMI) and naphthalene dicarboxymonoimide (NMI) as donors at the center, in the interior, and on the periphery, respectively.[29] Upon excitation of the exterior NMI moiety at 370 nm, **20** displays only weak emissions centered at 431 and 555 nm due to NMI and PMI, respectively. Instead, a strong emission is observed at 700 nm from the focal TDI unit, suggesting a two–step energy transfer from the NMI moiety to the focal TDI, through interior PMI chromophores.

From an application point of view, an important aspect is to integrate the light–harvesting antenna in an intermolecular energy transfer system. This concept has been demonstrated with a self–assembled monolayer of Coumarin 2–modified poly(aryl ether) dendron as light–harvesting segment in the presence of Coumarin 343 unit as energy acceptor unit.[30] Although the two components are randomly anchored on silicon wafer, intermolecular energy transfer from the dendron to Coumarin 343 unit takes place, where the ef-

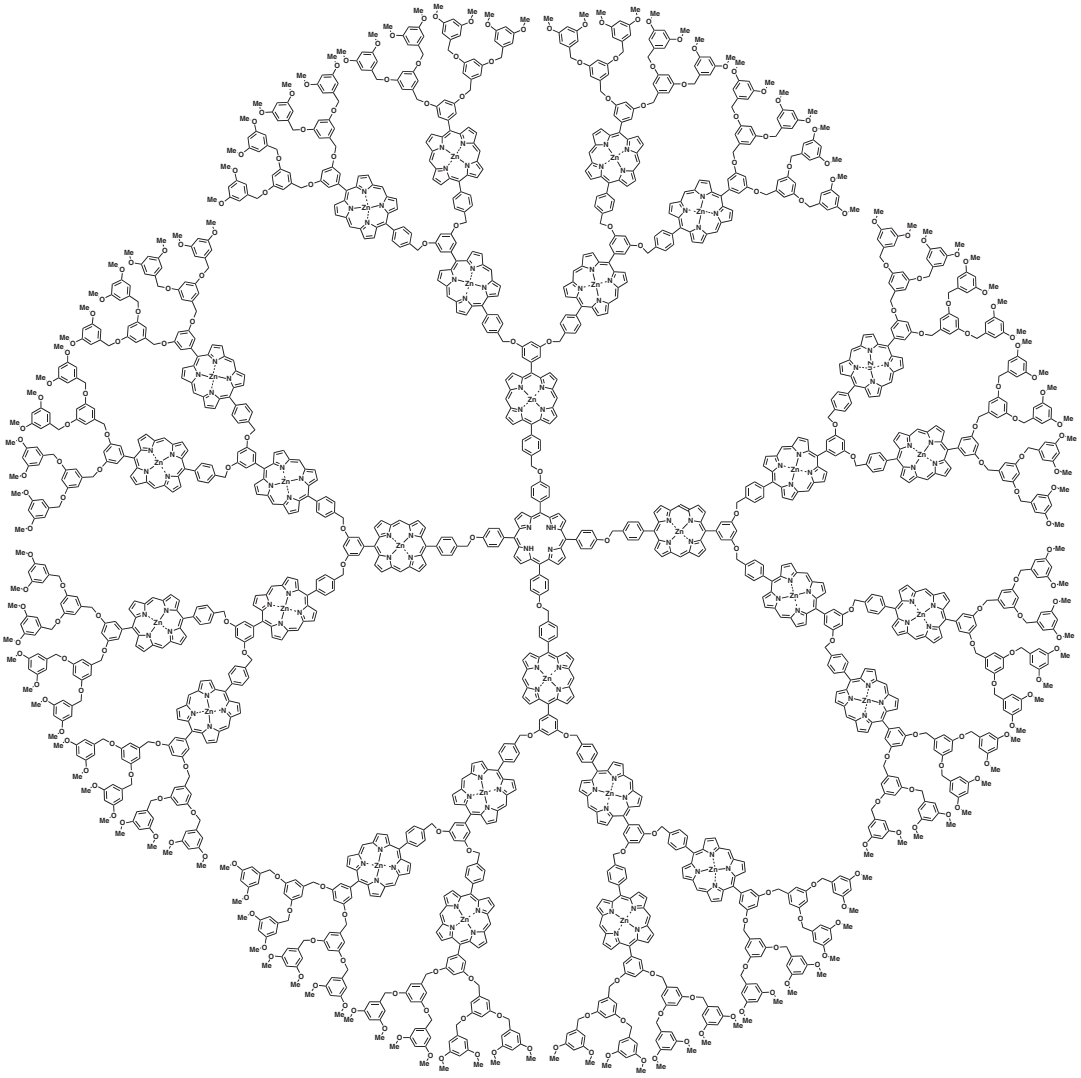

21

ficiency is highly dependent on the donor–acceptor molar ratio and the generation number of the dendron.

Antennae for Visible and Infrared Light Harvesting

As one of the strategies for the preparation of visible light–harvesting systems, multiporphyrin dendritic arrays[31–33] are among the most promising candidates to mimic the natural light–harvesting complexes because of their structural similarity. Multiporphyrin dendrimer **21**, with a spherical-shaped morphology, consists of a focal free–base porphyrin core as the acceptor surrounded by four dendritic wedges of zinc porphyrin heptamer as energy–donating units.[34] **21** upon excitation at 544 nm due to the zinc porphyrin units, emits a predominant fluorescence at 658 and 723 nm from the focal free–base porphyrin units, suggesting the occurrence of an efficient energy transfer from zinc porphyrin units to free–base porphyrin core. The energy transfer efficiency (Φ_{ENT}) and the energy transfer rate constant (k_{ENT}) have been evaluated to be 71% and $1.04 \times 10^9\ s^{-1}$, respectively. In contrast, compound **22**, a conical analogue of **21**, emits mainly from the zinc porphyrin units with only a weak emission from the focal free–base porphyrin core under identical conditions. The energy transfer in **22** is much less efficient as evidenced by its smaller Φ_{ENT} and lower k_{ENT} values of 19% and $0.10 \times 10^9\ s^{-1}$, respectively. Such a significant difference indicates that the morphology of the chromophore array in the dendrimer framework plays an important role in intramolecular energy transfer, as observed for the UV light–harvesting dendrimer porphyrins **1**–**6**. Excitation of spherical array **21** at 544 nm with polarized light gives a highly depolarized fluorescence spectral profile with an anisotropy of only 0.03. By contrast, conical analogue **22** shows a larger anisotropy value of 0.10. This indicates that the zinc porphyrin units in **21** can cooperate with one another within the four dendritic wedges, which facilitates the energy transfer to the focal free–base porphyrin core.

Detailed investigations on the light–harvesting properties of the morphologically different spherical

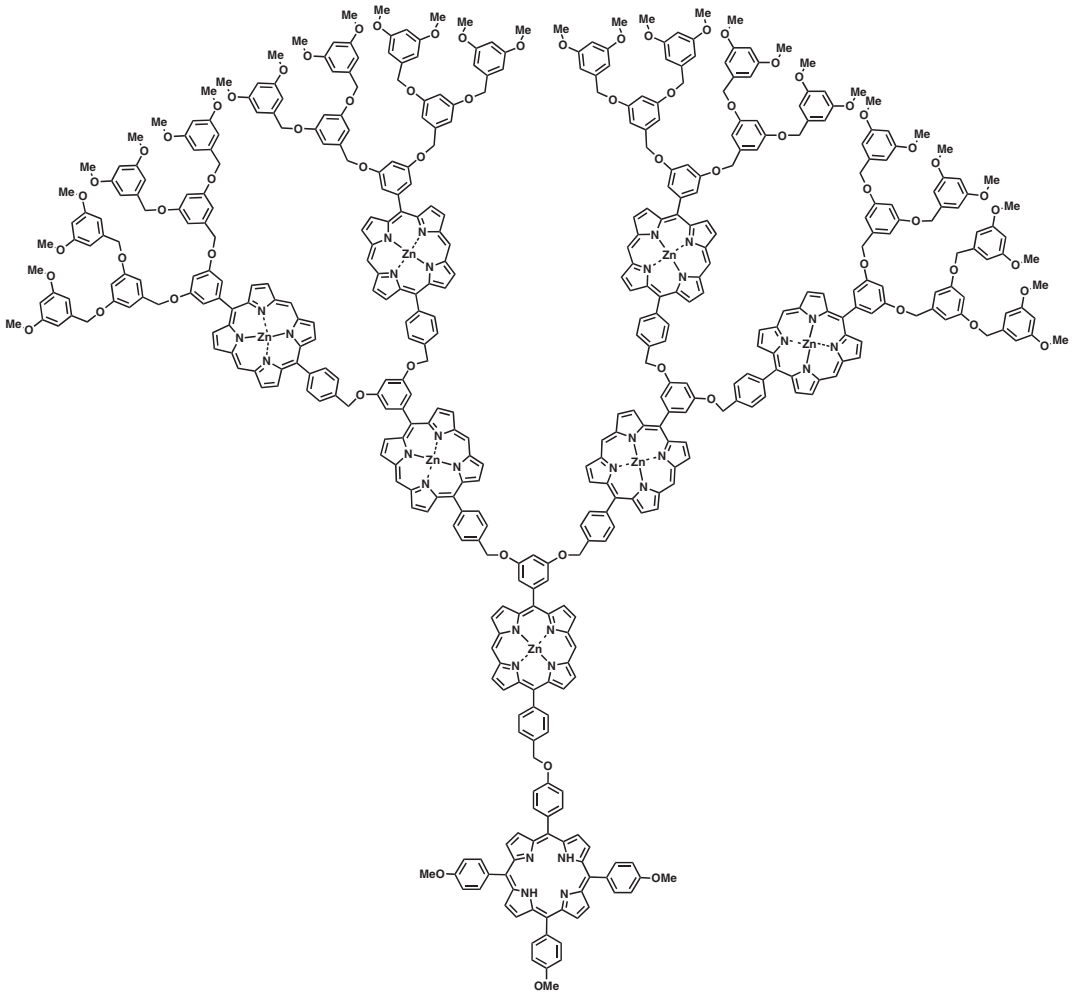

22

and conical dendrimers reveal that the two series of compounds display different generation–number dependency. As the generation number increases, the spherical series show only a slight decreasing in Φ_{ENT} value from 87% (**25**) to 80% (**23**), and to 71% (**21**).[35] On the other hand, the Φ_{ENT} value of the conical series significantly decreases from 86% (**26**) to 66% (**24**), and then to 19% (**22**) with increasing the generation number. The light–harvesting activities of spherical series, if termed as the multiple of absorption cross–section with the energy transfer efficiency, considerably increase with the generation number, whereas those of the conical series are much lower and less dependent on the generation number.[36]

Along this line, in order to elucidate the energy transfer process, Li and coworkers have synthesized hexaarylbenzene–anchored zinc(II) porphyrin dendrimers with 6 (**30**), 12 (**31**), 18 (**32**), 24 (**33**), and 36 (**34**) zinc porphyrin units on the exterior surface, as well as their constituent one– (**27**), two– (**28**), and three–branched (**29**) dendrons.[37,38] Steady–state absorption and fluorescence spectroscopy show that each zinc porphyrin moiety acts as an individual chromophore. One–branched **27** exhibits a single anisotropy decay with a rotational diffusion time of 320 ± 10 ps, while **30** shows an excitation energy transfer time constant of 542 ± 1 ps. AM1 Hamiltonian calculation based on the molecular geometry suggests that the six zinc porphyrin moieties in **30** are located in–plane with a two–dimensional circular geometry. Two–branched dendron **28** shows a fast excitation energy transfer time constant of 316 ± 2 ps, which is related to the conformer with short inter–chromophore distance. In agreement with its biexponential decay, two–branched dendrimer **31** with 12 zinc porphyrin units on the exterior surface, as optimized with AM1 Hamiltonian, adopts dual hexagonal wheels in a staggered conformation. Since the shortest distance between two chromophores located in different wheels is smaller than that within a same wheel, the fast anisotropy decay is attributable to inter–wheel and the slow component to intra–wheel excitation energy transfer processes. Accordingly, the experimental inter– and intra–wheel excitation energy transfer times are estimated as 24 ± 1 and 623 ± 15 ps, respectively. Larger dendrimer **33** bearing 24 zinc porphyrin

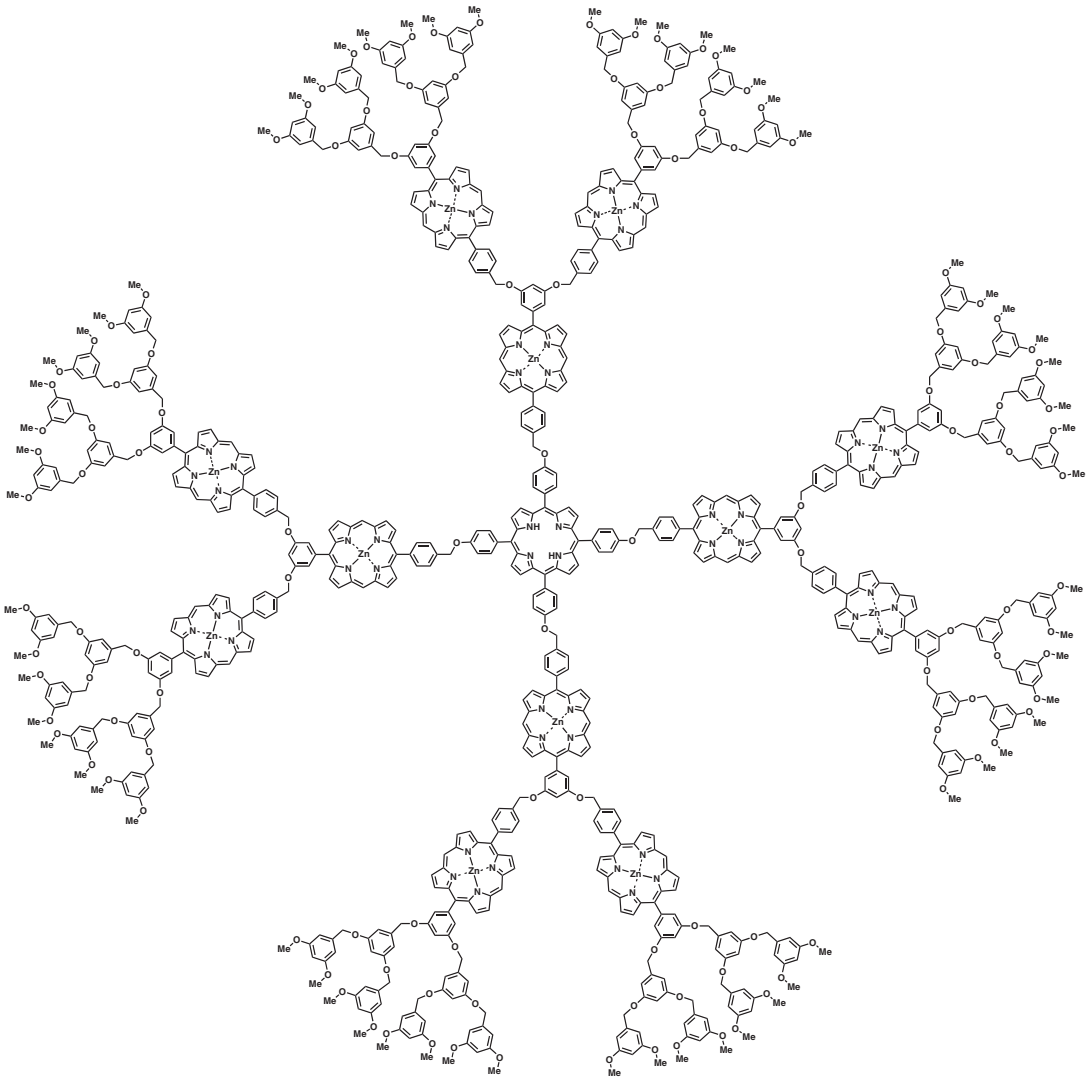

23

units on the exterior surface also shows biexponential anisotropy decay, which, however, is faster than that of **31** with 12 chromophores. Together with the fact of a similar rotation diffusion time of **33** to that of **31**, **33** with doubled numbers of zinc porphyrin units is likely to be a highly congested wheel with tightly packed zinc porphyrin units.

Compared to two–branched dendron **28**, the three–branched dendron **29** with a compact three–dimensional triangular structure, displays biexponential anisotropy decay and dual energy migration paths. The fast and slow components can be assigned to the excitation energy transfer times between neighboring and next nearest neighboring zinc porphyrin units, respectively. Three–branched dendrimers **32** and **34** exhibit biexponential anisotropy decays with similar time constants to those of dendron **29**. These features suggest that three–branched dendron **29** acts as a cluster in the excitation energy transfer processes because the zinc porphyrin units are already in close contact. The slow depolarization times of 900 and 740 ps observed for **32** and **34** are assignable to the inter–cluster excitation energy transfer process. Therefore, the fast excitation energy transfer process takes place in clusters and the slow one occurs between clusters. All these observations indicate that the excitation energy is not localized on a specific chromophore but can migrate over multiporphyrin arrays on the dendritic surface, where the energy transfer is highly dependent on the arrangement of chromophores.

In addition to above multiporphyrin dendrimers, dendrimer **35** bearing free–base porphyrin core, covalently linked with eight zinc porphyrin units, has been reported.[39] Excitation of zinc porphyrin units leads to an emission from the focal free–base porphyrin core, where a slow zinc porphyrin–to–free–base porphyrin energy transfer ($k_{ENT} = 9 \times 10^8\ s^{-1}$) takes place with Φ_{ENT} of 60%. A much larger multiporphyrin array **36**, which contains a free–base porphyrin at the focal core and 20 zinc porphyrin units in the branches, displays

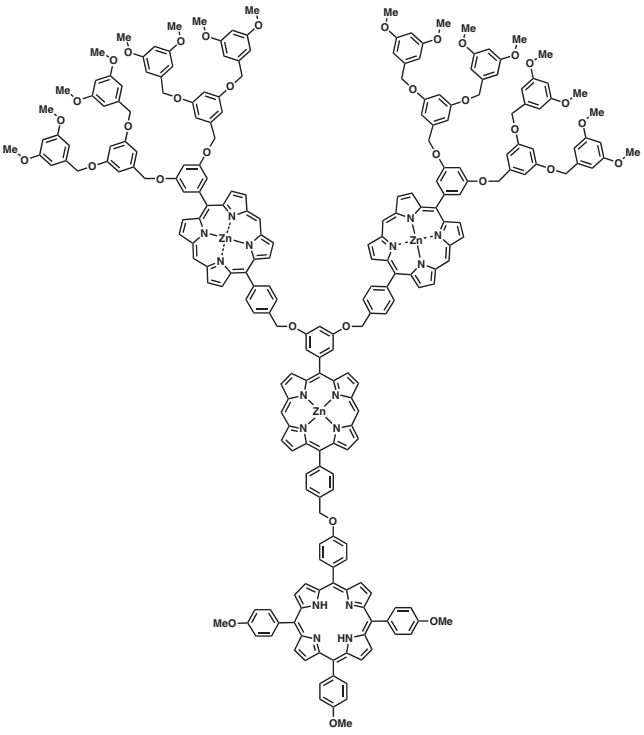

24

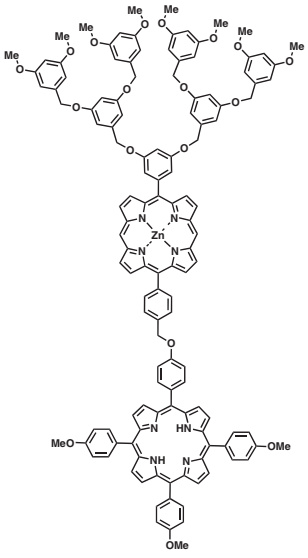

26

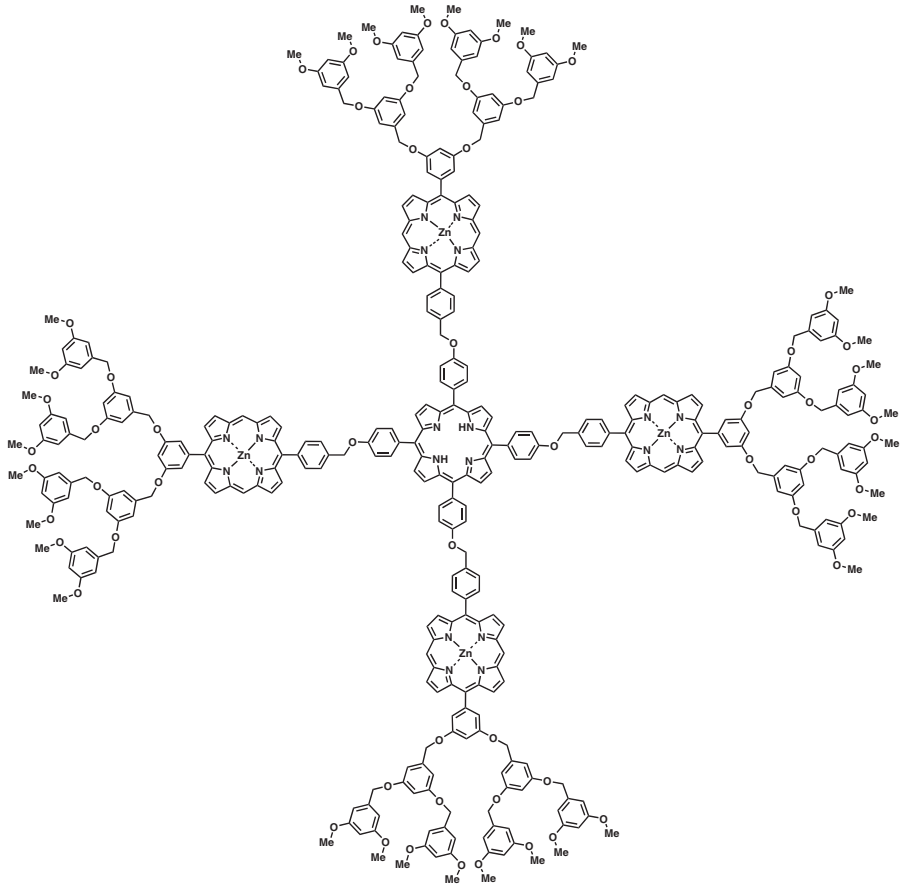

25

highly efficient energy transfer with Φ_{ENT} of 92%.[40]

As described above, single molecular approach allows for the synthesis of light–harvesting dendrimers capable of intramolecular vectorial energy transfer. Another aspect of equal importance is the utilization of dendritic macromolecule as a building block to fabricate light–harvesting supramolecular arrays.[41] Li, Wasielewski, and coworkers have synthesized a rigid

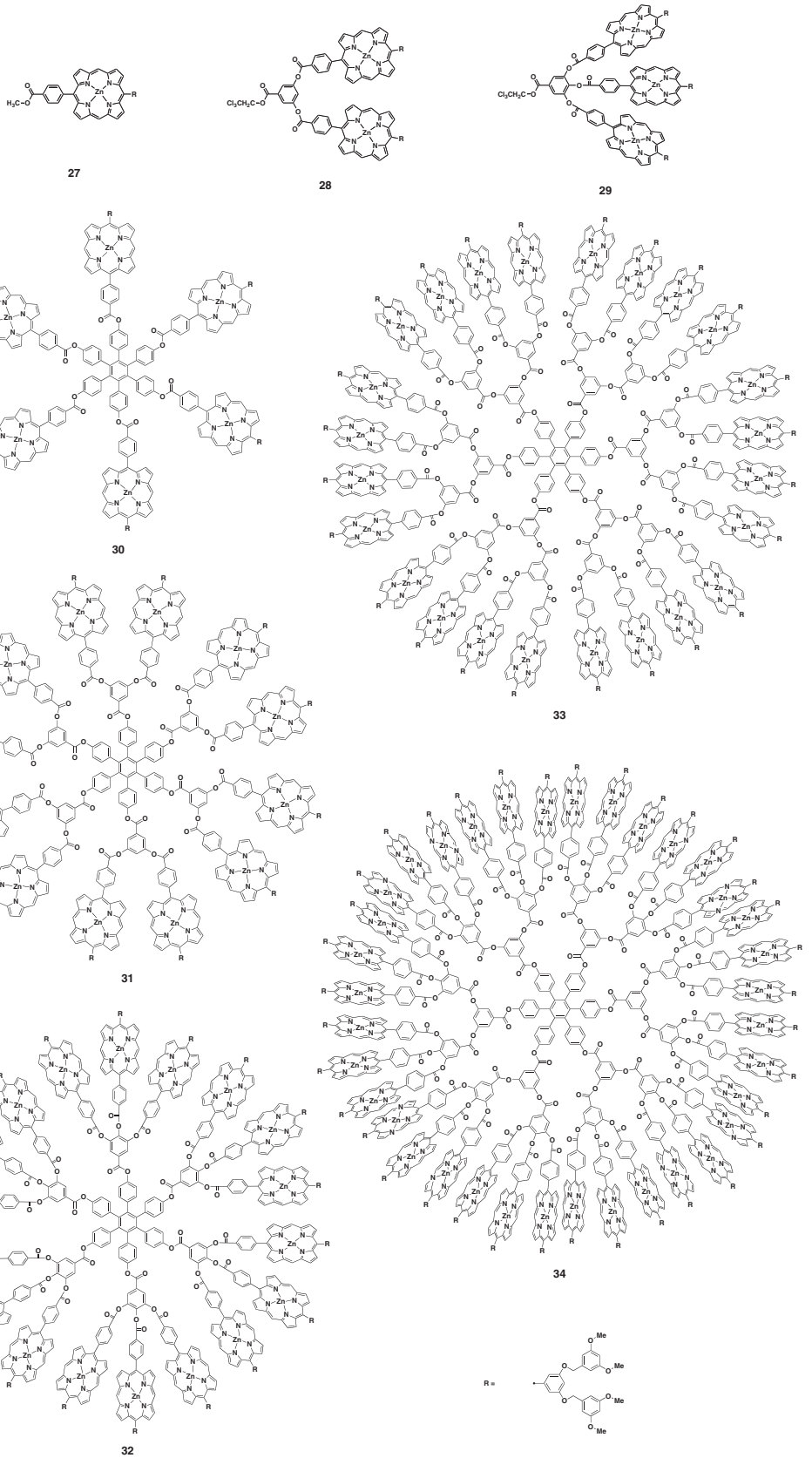

planar 'baby' dendrimer **37** having a zinc phthalocyanine (ZnPc) core tethered with four perylenediimide (PDI) units.[42–44] Electronic spectroscopy of **37** shows two broad bands at 500 and 645 nm due to PDI and ZnPc, respectively, both largely blue–shifted in relative to those of corresponding monomers, suggesting the formation of H–aggregates. Small–angle X–ray scattering measurement confirms that seven coaxially

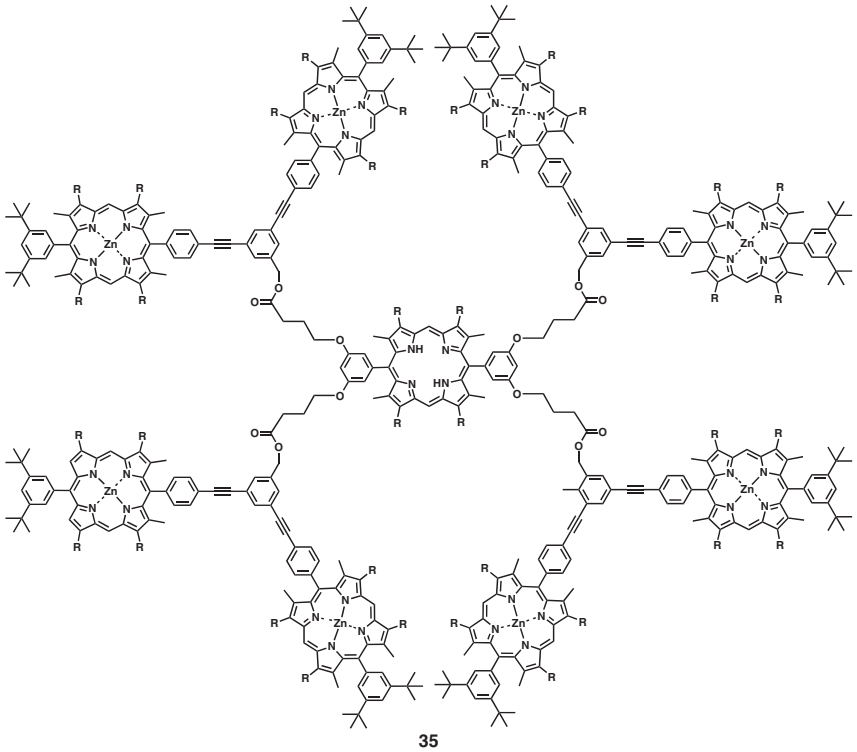

35

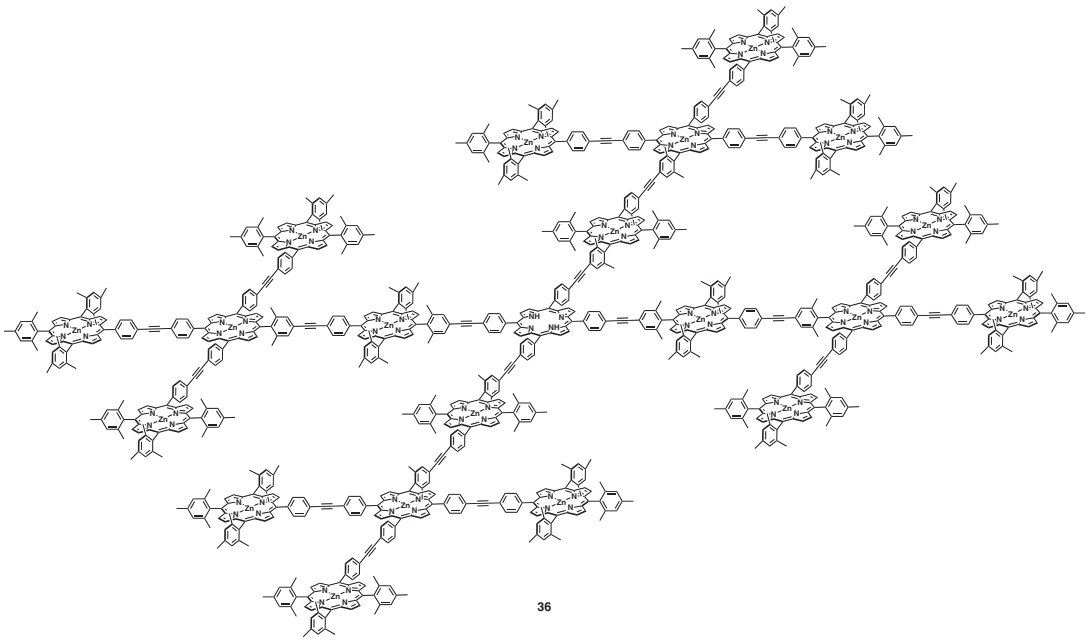

36

stacked molecules self–assemble into a stable cylindrical aggregate $(\mathbf{37})_{7mer}$ with an overall dimension of $6 \times 6 \times 3$ nm. Selective excitation of the peripheral $(PDI)_{7mer}$ in $(\mathbf{37})_{7mer}$ at 500 nm results in the formation of single excitation state of $(PDI)_{7mer}$, which undergoes quantitative singlet–singlet energy transfer to the focal $(ZnPc)_{7mer}$ column, followed by the formation of singlet excitation state of $(ZnPc)_{7mer}$ with a lifetime of 1.3 ps.

Unlike UV and visible light, low energy photons in the IR region is easy to dissipate to surroundings and hardly transfer to a designated site. A poly(benzyl ether) azodendrimer **38** carrying photoresponsive azobenzene core have been synthesized.[45,46] Of interest, *cis* form of **38** in $CHCl_3$ isomerizes to the *trans* form, when exposed to an IR light of 1597 cm^{-1}, corresponding to the vibrational band of the aromatic rings in the dendrimer framework, whereas no acceleration occurs in low–generation dendrimers or mono–dendritic analogues. The large dendritic shell not only serves as an insulator to prevent collisional energy dissipation, but also functions as an IR light–harvest-

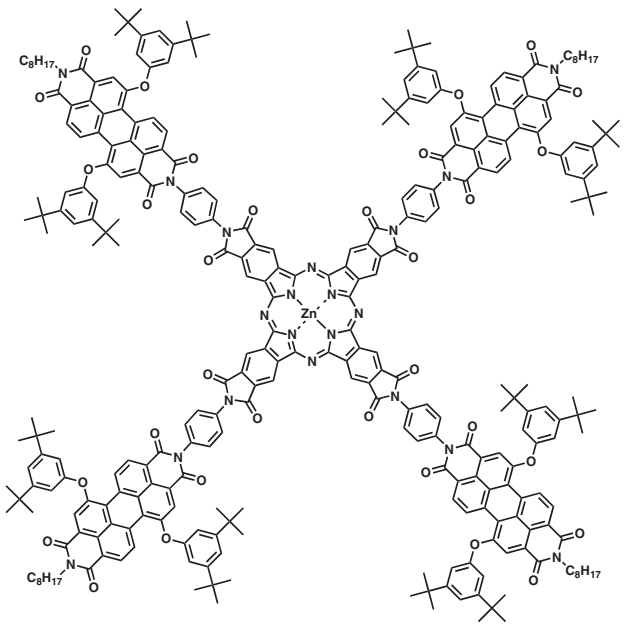

37

ing antenna. Such an intriguing IR effect has been investigated by Mo and coworkers with Raman spectroscopy of a dendritic iron porphyrin complex (**1**).[47] Upon IR irradiation of the dendrimers in dioxane at 1597 cm^{-1} due to aryl ν_8 mode of the aryl ether dendrons, the Boltzmann temperature of metalloporphyrin vibrational modes including axial Fe–Cl stretching mode at 355 cm^{-1} (T_{355}) and porphyrin in–plane mode at 390 cm^{-1} (T_{390}) is higher than that of the solvent (T_{835}). While T_{835} of neat solvent remains unaffected by IR irradiation, the differential temperatures, ΔT_{355} defined as T_{355}–T_{835} and ΔT_{390} as T_{390}–T_{835}, increase with increasing the generation number and IR intensity. For high–generation dendrimers, ΔT_{355} of Fe–Cl stretching is always larger than ΔT_{390} of porphyrin in–plane mode. These results demonstrate that the IR energy captured by the ν_8 mode of the aryl dendritic antenna is most likely transferred to the axial Fe–Cl bond of the Fe–porphyrin core and then relaxed to the porphyrin macrocycle.

Antennae for Two–Photon Absorption

Molecular design of two–photon absorption (TPA) systems has attracted much attention due to their potential utilities in diverse fields such as photodynamic therapy of cancer, fluorescence microscopy, and optical power limiting.[48–51] One attractive way to enhance TPA cross–section is to design a polymer containing a large number of TPA units without causing any aggregation of chromophores. In this sense, dendritic macromolecules emerge as promising candidates, since their unique three–dimensional scaffolds can accommodate many TPA chromophores and have a chance to increase significantly the molecular absorption cross–section.

Since **39** is a well–established TPA chromophore with a large TPA cross–section of 6,700 (±15%) GM (1 GM = 10^{-50} cm^4 s) at 800 nm, Adronov and Fréchet have employed **39** derivative for the synthesis of a series of TPA–dendrimers **40**–**42** with different generation numbers.[52] As the generation number increases, the TPA cross–section of dendrimers increases proportionally to show a linear correlation with the number of the chromophores. Based on this observation, nile red chromophore has been anchored at the

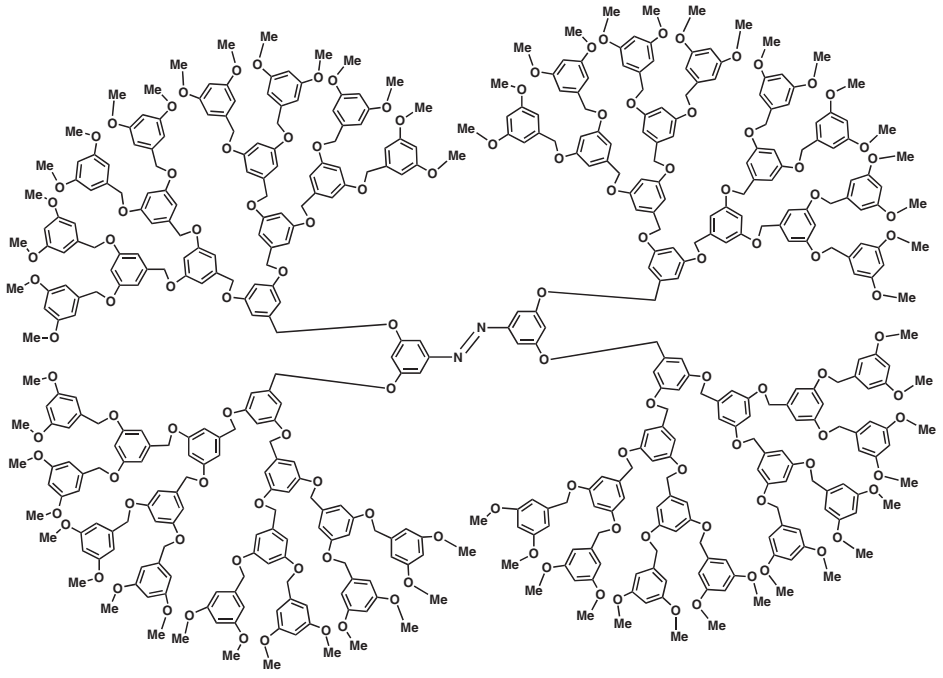

38

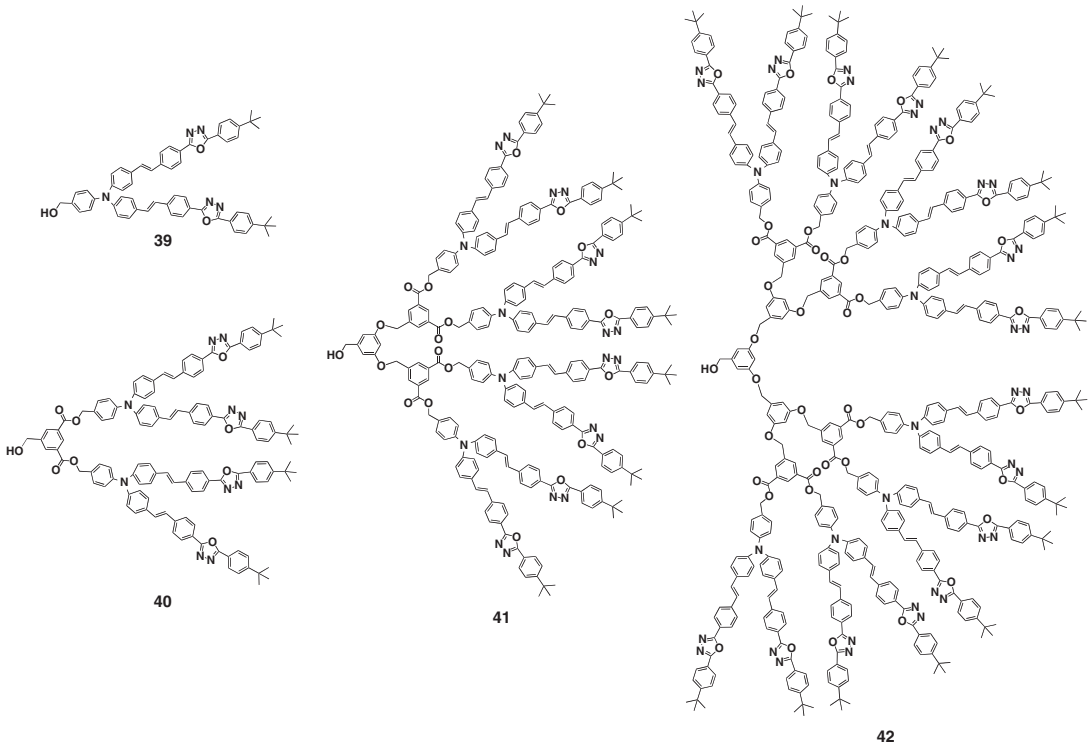

focal core of a series of dendrons bearing **39** units on the exterior surface to give dendritic nile red (**43**–**45**). Two–photon excitation of **43**, **44**, and **45** with 815–nm laser leads to an emission at 595 nm from the nile red core, whose intensity is increased by 8, 20, and 34 folds compared to that upon excitation of nile red itself at the same wavelength, respectively.[53,54] The TPA cross–sections of **43**–**45** double from 6,700 (±15%), to 11,900 (±15%), and then to 24,100 (±15%) GM, while the number of TPA moieties increases from one, to two, and then to four.

Porphyrin derivatives are well–known as photosensitizers for activation of oxygen to generate singlet oxygen with high quantum yield, which is attractive as potential agents for photodynamic therapy (PDT).[55–57] However, ordinary porphyrins show absorption for UV and visible light, which have only limited transmission through skin. From a PDT point of view, porphyrin derivatives capable of absorbing near–IR such as 750–1,000 nm lights, which reach much deeper tissues, is highly required. To challenge this subject, a promising way is to combine a TPA antenna with a dendritic porphyrin photosensitizer. Fréchet and coworkers have designed and synthesized a dendritic porphyrin **46** containing eight TPA units, *i.e.*, AF 343 moieties on the surface.[58] AF 343 has been chosen as an energy–donating unit because of its high TPA cross–section and large emission spectral overlap with porphyrin absorption band. Upon two–photon excitation of AF 343 units with a 780–nm fs–mode locked Ti:Sapphire laser, **46** emits a fluorescence from the focal porphyrin core with an intensity 17 folds that of the simple porphyrin reference **47**, indicating that AF 343 units can efficiently harvest and transfer the two–photon excitation energy to the focal porphyrin core. Two–photon excitation of **46** in oxygen–saturated solution at 780 nm affords a fluorescence at 1,270 nm characteristic of singlet oxygen, whereas **47** does not show any emission under identical conditions. Therefore, the near IR energy harvested by AF 343 units on the exterior surface of the dendrimer framework is channeled to the focal porphyrin core and can be utilized in the generation of singlet oxygen. In fact, a water–soluble version, **48**, tethered with tri(ethylene glycol) monomethyl ether groups on the surface, allows the generation of singlet oxygen in aqueous solution upon two–photon excitation at 780 nm.[59] Such a water–soluble dendrimer capable of near IR excitation is highly interesting from an application point of view. A water–soluble poly(arylglycine) dendritic platinum porphyrin **49** bearing Coumarin–type TPA chromophores has been developed as a phosphorescent probe for the imaging of tissue oxygen, based on a similar photoinduced energy transfer reaction.[60,61]

DENDRITIC ARCHITECTURES FOR PHOTOINDUCED ELECTRON AND HOLE TRANSFER

Unlike traditional linear, star–shaped, and branched polymers, dendritic architecture is characterized by its

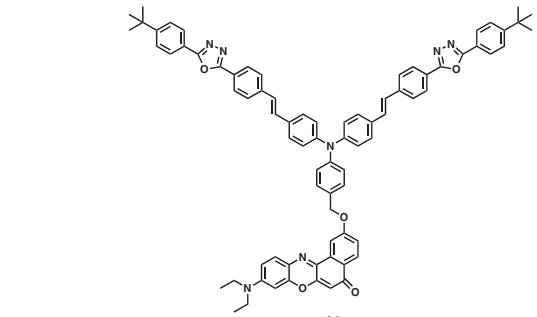

43

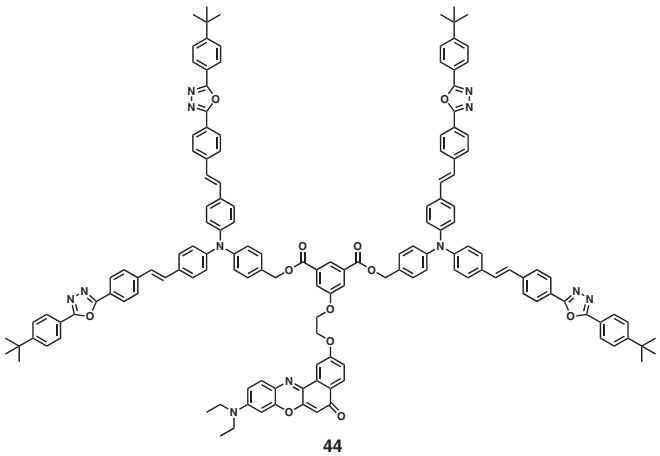

44

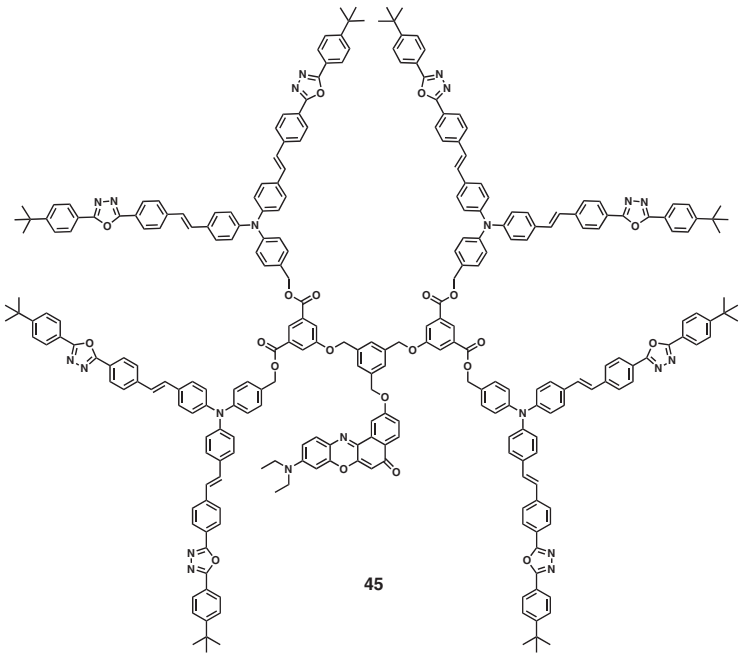

45

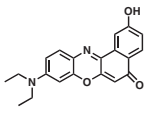

nile red derivative

elaborative molecular design capability, especially for site–specific placement of electron donor and acceptor components in the three–dimensional scaffold, thus provides a well–defined molecular system for the photoinduced electron and hole transfer. Covalent and non–covalent approaches have been developed for the construction of photoinduced electron–transferring (PET) systems based on dendritic architectures. In both cases, the dendrimer framework serves as a medium for regulating the photoinduced electron transfer reaction and the stability of resultant charge–separation (CS) state.

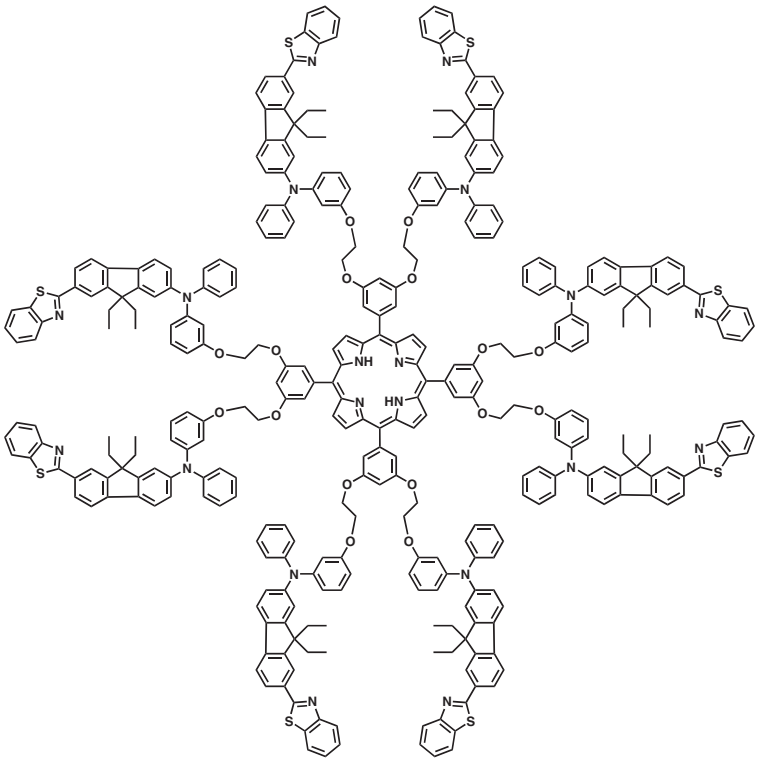

46

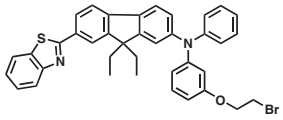

AF-343

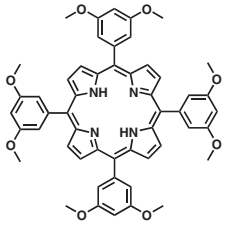

47

Porphyrin–Based Dendritic PET systems

In the natural photosynthetic reaction center, multi–step electron transfer reactions, mediated by porphyrin derivatives, play a crucial role and the resulting charge–separation state between the special pair and end quinone group generate chemical potentials from photo–energy. To accomplish an artificial photosynthesis, a huge number of multi–porphyrin systems bound to an electron acceptor have been synthesized and the photoinduced charge–separation states have been well investigated.[62] In particular, dendrimers consisting of porphyrin moieties as electron–donating groups coupled with various electron acceptors have been synthesized for the investigation of photoinduced electron transfer event with an aim to achieve long–lived charge–separation state.

By encapsulating a zinc porphyrin unit at the core of a carboxyl–terminated poly(benzyl ether) dendrimer framework, Sadamoto and Aida have demonstrated the photoinduced electron transfer from porphyrin core to a positively charged electron acceptor, *i.e.* methyl viologen (MV^{2+}), which is electrostatically self–assembled on the surface of the dendrimer framework.[63] The photoinduced electron transfer event is highly dependent on the generation number of the dendrimer framework. In contrast to the 1st–generation dendrimer **50**, the 3rd–generation dendrimer **51** in a phosphate buffer, upon titration with MV^{2+}, exhibits higher degree in fluorescence quenching, indicating a much more efficient photoinduced electron transfer. The rate constant of the photoinduced electron transfer has been estimated as $2.6 \times 10^9\ s^{-1}$. Therefore, the pre–organized electron donor–acceptor array, which is spatially separated by the large dendrimer framework, shows an efficient photoinduced electron transfer from the focal core to MV^{2+} through the 2–nm thick dendrimer framework. The large dendrimer framework prevents the photoactive core from aggregation, and thus greatly lowers the possibility of collisional dissipation of the photoexcited state.

Fréchet and coworkers have synthesized a series of poly(benzyl ether) dendrimer zinc porphyrins to show the site–isolation effect on the focal zinc porphyrin unit.[64] High–generation dendrimer **52** exhibits a lower activity in electron transport from/to electrode, as evidenced by a larger redox potential. However, the large dendrimer framework does not restrict the access by small molecules. For example, upon addition of benzylviologen as an electron acceptor, **52** shows even an enhancement by 33% in the photoinduced electron transfer rate.

In contrast to the self–assembled donor–acceptor array, Modarelli and coworkers have developed a covalently linked system, by appending electron acceptor, *i.e.* anthraquinone to the exterior surface of polyamide dendrimer porphyrins.[65] In this case, both fluorescence quenching degree and photoinduced electron transfer rate retain at similar level, irrespective of the generation number. Although the largest dendrimer **53** bearing 108 anthraquinone groups on

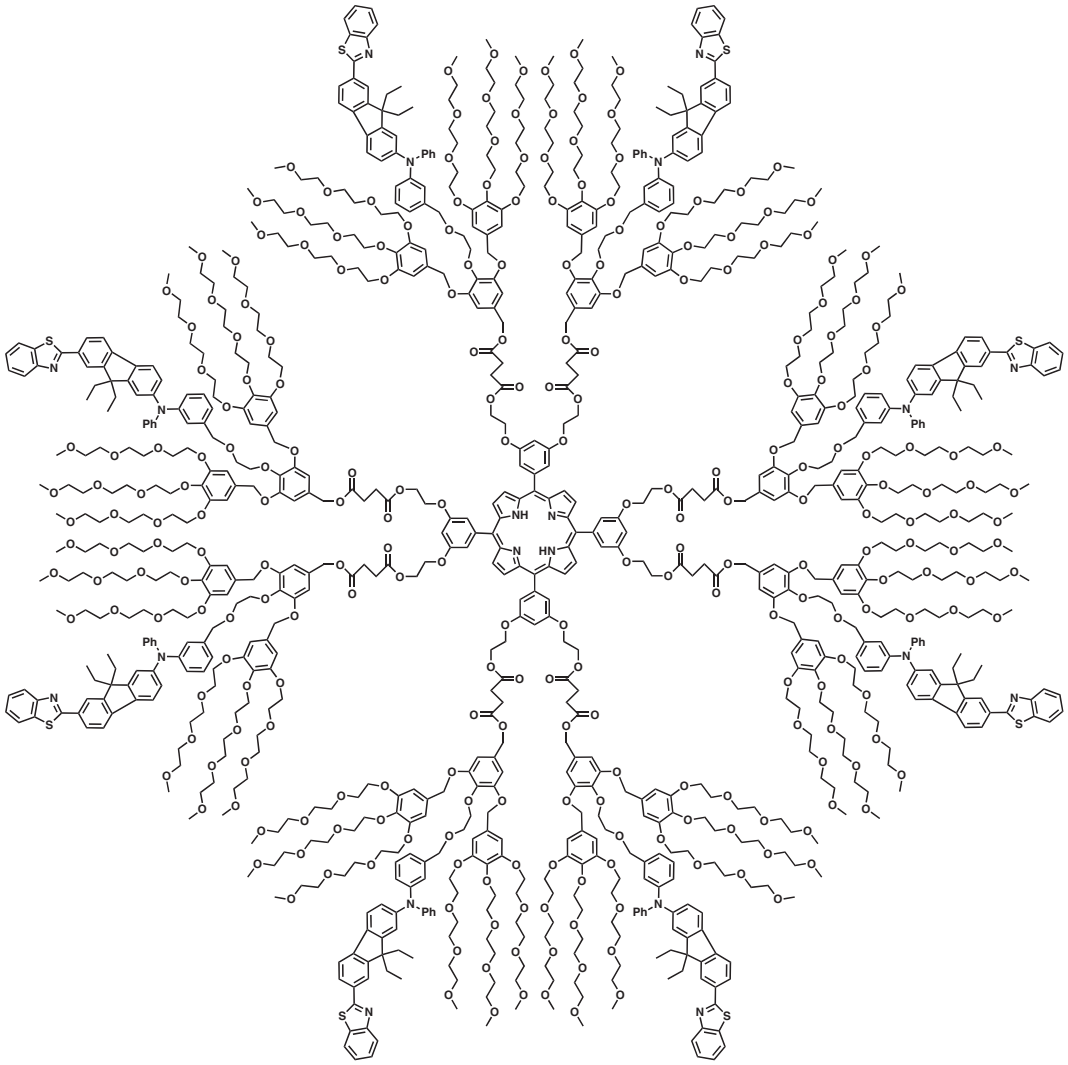

48

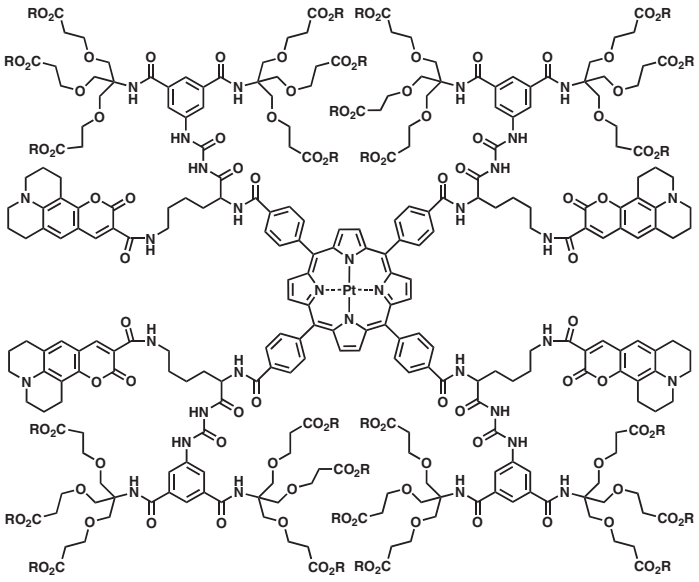

49
R = ^{t}Bu or H

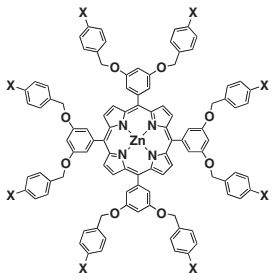

50
X = CO_2^-

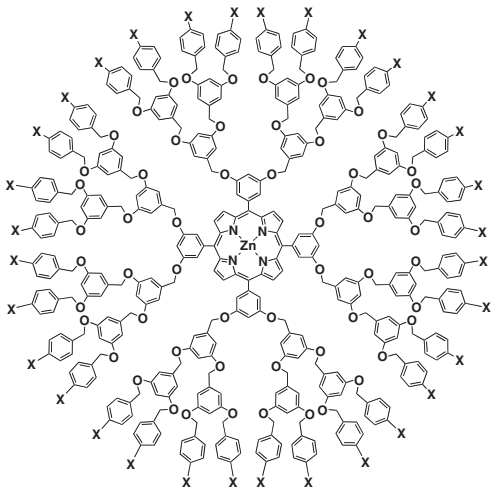

51
X = CO_2^-

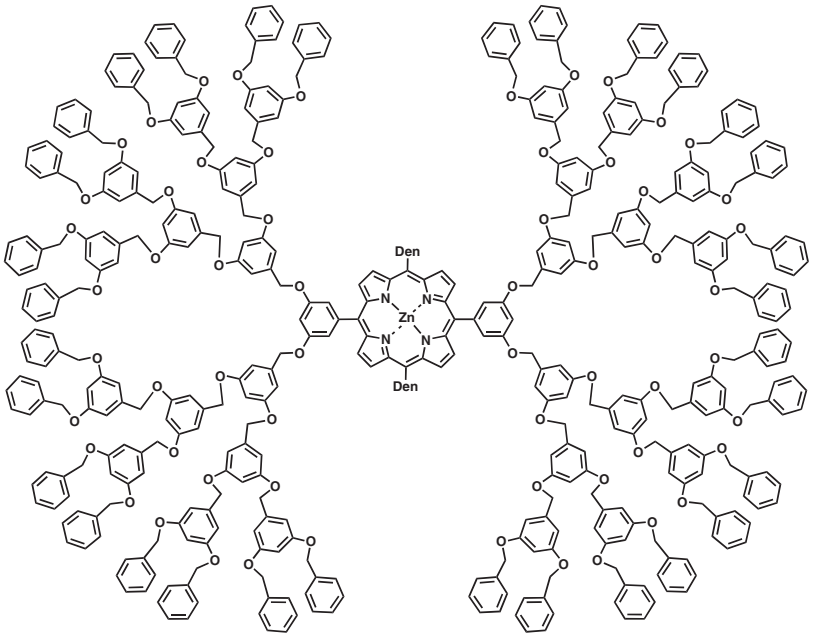

52

the exterior surface, it exhibits a fluorescence quenching degree of only 60%. The low fluorescence quenching efficiency is likely owed to the distance between donor and acceptor as long as 2.6 nm, which is close to the spatial limit for a through–space electron transfer reaction.

Porphyrin–fullerene dyads have attracted much attention as novel photoinduced electron transfer units, in which the charge–separation state can take advantage of the low reorganization energy of fullerene. In 1999, Hirsch and coworkers have reported fullerene–porphyrin dyads with different numbers of poly(benzyl ether) dendritic wedges anchored on the fullerene moiety.[66] As the number of dendritic wedges increases, the fluorescence quenching becomes less efficient, as a result of the decrement of π–electron acceptability for substituted fullerene.

The integration of dendritic light–harvesting antenna in electron–transfer relay systems is of interest due to the high probability for triggering vectorial energy flow and electron–transfer process. Choi, Aida, and coworkers have reported the pioneering work on the synthesis of a series of fullerene–terminated dendritic zinc porphyrin arrays, **54**–**56**, consisting of one, three, and seven zinc porphyrin units as light–harvesting moieties.[67] Average fluorescence–decay rate constant (k_{CS}) becomes smaller by a factor of four as the zinc porphyrin array becomes larger from **54** ($1.55 \times 10^9\ s^{-1}$) to **55** ($0.40 \times 10^9\ s^{-1}$). **56** shows a k_{CS} value of $0.43 \times 10^9\ s^{-1}$, which is comparable to that of **55**,

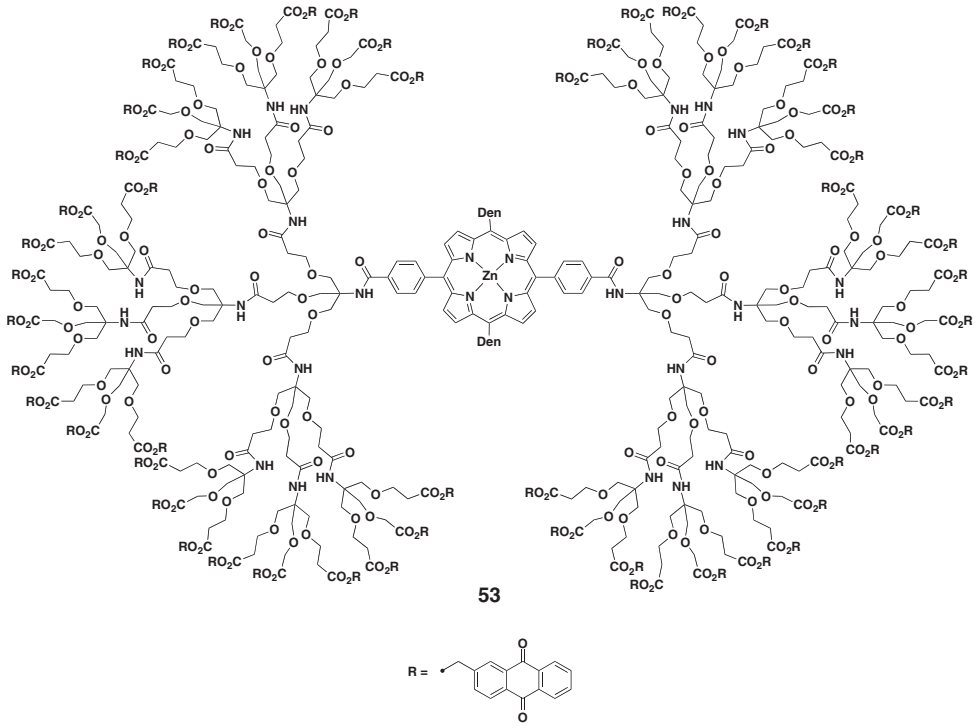

although **56** bears a larger number of zinc porphyrin units located away from the fullerene terminus. Similarly, the quantum efficiency for charge separation (Φ_{CS}) of **56** has been estimated as 51%, which is smaller than that of **54** (80%) but comparable to that of the lower–generation **55** (49%). Interestingly, the largest, **56**, shows a smaller charge–recombination rate constant ($k_{CR} = 1.5 \times 10^6\ s^{-1}$) than those of **54** ($2.9 \times 10^6\ s^{-1}$) and **55** ($2.4 \times 10^6\ s^{-1}$). Thus, the zinc porphyrin cationic radical species, which is initially generated at the focal point, can move away from the fullerene anionic radical terminus towards the periphery by intramolecular hole hopping. The large dendritic antenna not only harvests visible light for electron transfer to the fullerene terminus, but also retards the back electron–transfer process, thus indicating a new potential of dendritic macromolecules for conversion of light energy into chemical potentials.

Self–assembled biological structures, such as cell membranes formed from amphiphilic lipids and proteins, are of great interest in relation to their dynamic transportation of ions and molecules, and the transfer of energy across the membranes. Inspired by this elaborate natural system, the development of novel vesicular self–assemblies, especially in the creation of new functional artificial systems, has evolved as an important subject. Charvet and coworkers have reported that a zinc porphyrin–fullerene amphiphile **57** self–assembles to form photoactive vesicles.[68] Dynamic light–scattering analysis of **57** in a mixture of THF and water shows that the vesicles are uniformly–sized with 100 nm in diameter on average. Scanning electron microscopy and TEM reveal the formation of core–shell spherical particles with a shell thickness of 25–30 nm, indicating that they consist of a multilamellar membrane.

A long tailing in the near–IR region (650–1,000 nm) in the electronic absorption spectrum is characteristic of charge–transfer π–electronic interactions between zinc porphyrins and fullerene. This suggests that the multilamellar membrane has an interdigitated structure, in which the fullerene moieties are sandwiched by the zinc porphyrin units. The fluorescence is completely quenched by fullerene units when **57** is interdigitated in the vesicles, since electron transfer takes place intermolecularly as well as intramolecularly in the vesicular membrane.

Li and coworkers have recently reported multiporphyrin–multifullerene arrays self–assembled from multiporphyrin dendrimers (**30**, **31**, and **33**) and fullerene–tethered bipyridine derivatives (**58**–**60**).[69] Time–resolved fluorescence spectroscopy of **33** gives a decay profile at 590 nm with a lifetime of 300 ps upon addition of fullerene–free bipyridine and a much faster decay with a lifetime of 150 ps in the presence of **60**. Of interest, as the generation number increases, the k_{CS} values of **30**, **31**, and **33** in combination with **60**, increase from 0.57×10^{10} to 1.5×10^{10}, and to $2.3 \times 10^{10}\ s^{-1}$. This generation–dependent increasing tendency is also observed for the combinations with **58** and **59**. On the other hand, the k_{CR} values are similar to one another around $6.7 \times 10^6\ s^{-1}$. Therefore, the k_{CS}/k_{CR} values, corresponding to the lifetime of the charge–separation state, increase with increasing

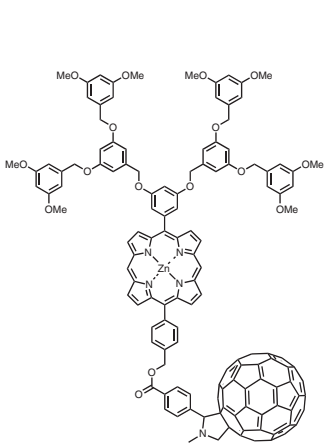

54

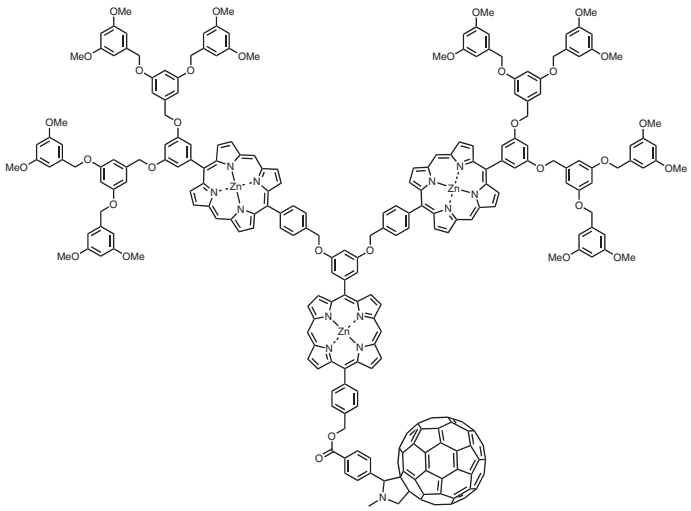

55

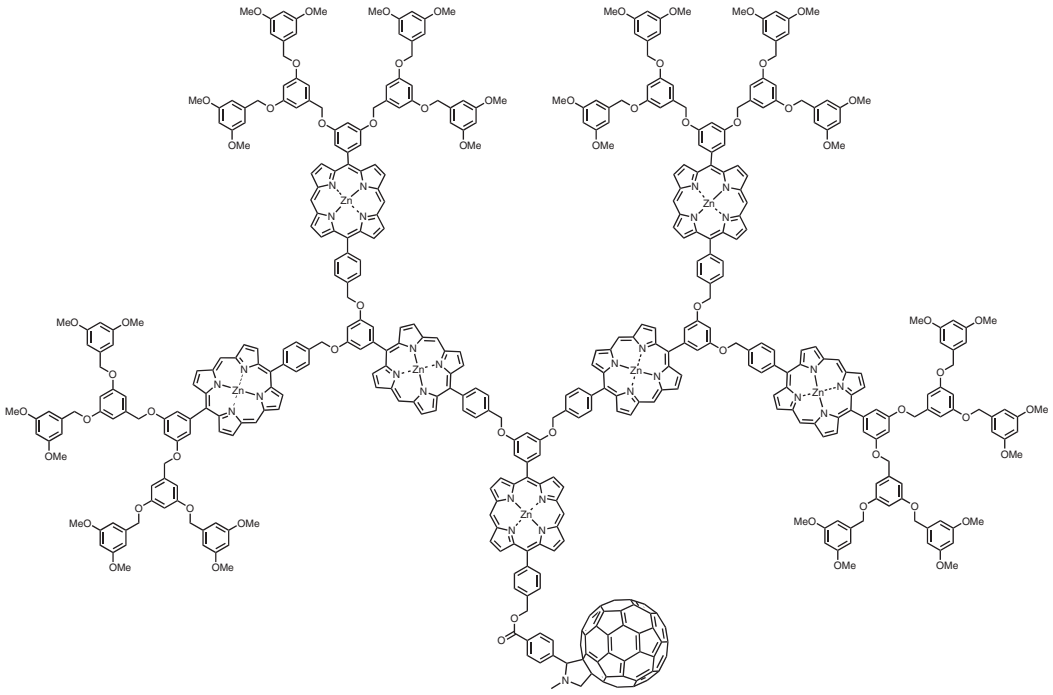

56

the generation number of the multiporphyrin dendrimers as well as the number of fullerene units. The largest multiporphyrin dendrimer **33** in conjunction with the largest multifullerene **59** shows the largest k_{CS}/k_{CR} value as 3,400 among the family. The increasing tendency of k_{CS}/k_{CR} values suggests that excitation energy may migrate over the multiporphyrin array and facilitates the photoinduced electron transfer.

Instead of fullerene derivatives, single–walled carbon nanotube (SWNT) has been used as an electron acceptor by Campidelli, Prato, and coworkers for the construction of a hybrid **61** bearing multiporphyrin poly(amidoamine) dendrons as an electron–donating group.[70] The dendrimer framework serves as a bulky spacer for spatial separation of porphyrin units from SWNT and prevents direct π–π interactions between porphyrin and SWNT. Thus, the photoinduced electron transfer reaction takes place from porphyrin units to SWNT and thereby leads to the generation of charge–separation state.

α–Helical oligopeptide chains, each containing one histidine unit as an axial ligand, have been introduced to the surface of polyamidoamine dendrimers and utilized for the assembly with zinc porphyrin to form supramolecular multiporphyrin arrays on the surface.[71] Due to the presence of positively charged arginine units in the oligopeptide chains, negatively charged acceptor such as naphthalene sulfonate induces a

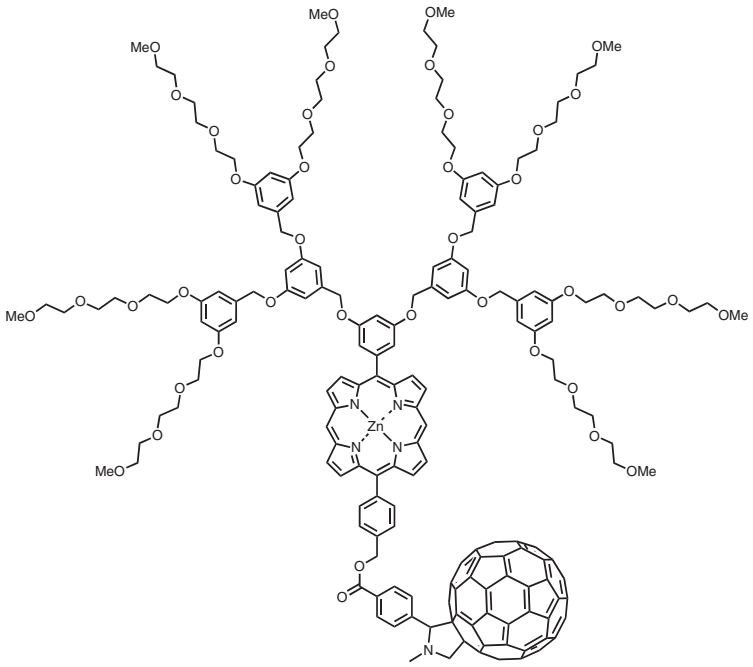

57

higher fluorescence quenching degree than that of positive one, *i.e.* MV^{2+}. As the generation number increases, the fluorescence quenching degree of multiporphyrin arrays increases. Based on this result, Mihara and coworkers have fabricated a four–component hydrogenase–mimicking system with MV^{2+} as an electron acceptor, triethanolamine as a sacrificed electron donor, for the photoinduced hydrogen evolution form water in the presence of hydrogenase as the redox catalyst.[71b] Based on a similar dendrimer, utilization of iron(III) porphyrin in couple with hydrogen peroxide as an oxidant allows for the construction of an artificial system mimicking the activity of peroxidase.[71c]

Due to the possibility for mediating hole and/or electron migration, DNA and its intercalation derivatives with chromophores such as porphyrin have attracted much attention as a motif for fabrication of photofunctional devices. Ikeda and coworkers have reported a photocurrent generator assembled on ITO electrode, by using DNA/porphyrin composite as electron donor, polyamidoamine dendrimer as stationary phase, and poly(vinyl sulfonate) or poly(allyl amine) as a supporting membrane.[72] As the generation number increases, the photocurrent increases to give an overall quantum yield of about 1% for the 4th–generation poly(amidoamine) dendrimer. To enhance photocurrent and quantum yield is yet a key point for further challenge.

Dendritic Conjugated Polymers for PET

Photoinduced hydrogen evolution from water has attracted much attention and has been considerably investigated in relation to solar energy conversion, for which organic dyes have been utilized as photosensitizers. Conjugated polymers with extended π–electronic conjugation are promising as photosensitizers, as they have large absorption cross–sections, show tunable light–absorbing properties, and allow exciton and hole migration along the backbone. However, their photosensitization activity remains unknown, owing to their insolubility in water and the strong tendency towards self–quenching of the photoexcited states. In order to explore the photosensitization effect of π–conjugated polymers and their activity in photoinduced hydrogen evolution from water, Jiang, Aida, and coworkers have synthesized a series of water–soluble conjugated polymers, **62–69**, wrapped with poly(benzyl ether) dendrimer frameworks bearing charged exterior surfaces.[73]

Upon excitation at 420 nm of the conjugated backbone, **64** in an aqueous Tris–HCl buffer (pH 7.4; 5 mM) emits an intense blue fluorescence centered at 461 nm with a Φ_{FL} value of 57%. In contrast, the smallest homologue **62**, emits at a longer wavelength of 521 nm with a Φ_{FL} value of only 7%. This is also the case for one–generation higher **63**, which forms excimer (521 nm) to give a low quantum yield of 29%. Therefore, the large dendrimer framework (2– nm thick) of **62** is effective in encapsulating the conjugated backbone even in water and preventing the loss of its excitation energy from the excimer formation. The addition of a cationic acceptor, *i.e.* MV^{2+} results in a significant decrease in the fluorescence in-

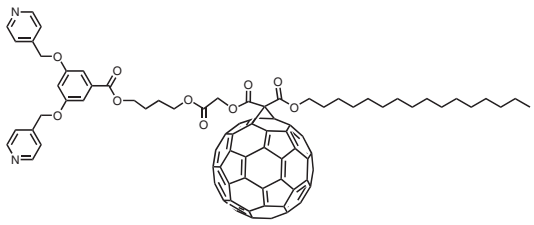

58

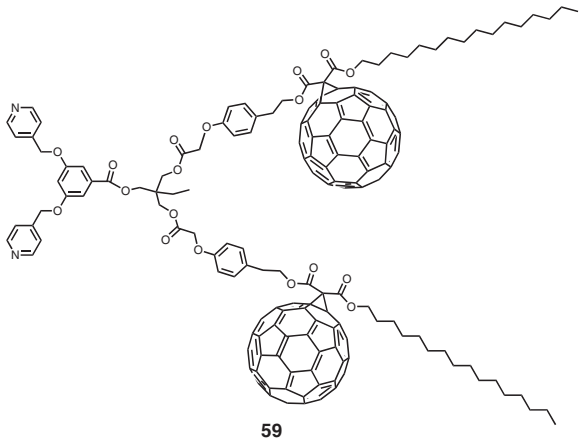

59

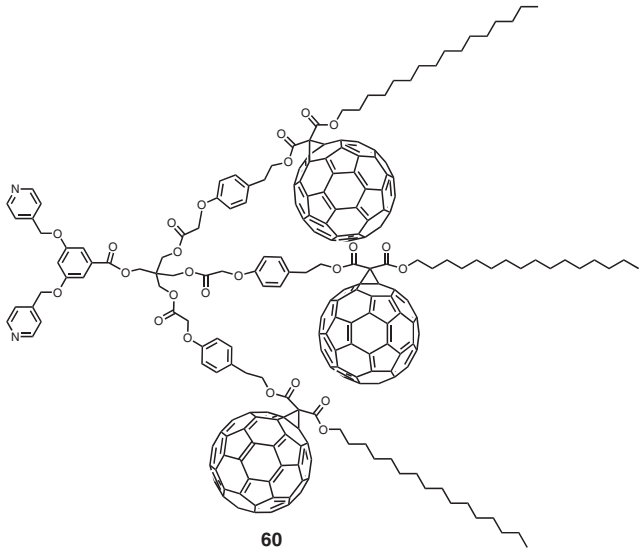

60

tensity of **64**, even at a low $[MV^{2+}]$ of 2.6×10^{-8} M, indicating that photoinduced electron transfer to MV^{2+} takes place efficiently from the conjugated backbone, although it is embedded in the large dendrimeric shell.

Time–resolved fluorescence spectroscopy shows that the lifetime of the fluorescence of **64** (880 ps) is considerably shortened to 96 ps in the presence of MV^{2+} (7.8 μM), where the rate constant for the electron transfer (k_{ET}) from **64** to the trapped MV^{2+} molecule is estimated to be $9.3 \times 10^9\ s^{-1}$. This k_{ET} value is sufficiently large, assuming a 2–nm thickness for the dendrimeric shell of **64**. The quenching–rate constant (k_q), as given by $((\tau_{ave}\ (acceptor))^{-1} - (\tau_{ave}\ (none))^{-1})/[MV^{2+}]$, is evaluated as $1.2 \times 10^{15}\ M^{-1}\ s^{-1}$, which is considerably larger than ordinary diffusion–controlled quenching rate constants (10^9–$10^{10}\ M^{-1}\ s^{-1}$). These observations indicate that the electron transfer takes place within the pre–organized supramolecular complex between **64** and MV^{2+}. A control experiment with the *meta*–linked **69**, which has a molecular weight almost identical to that of **64**, shows a K_{SV} value of only $2.0 \times 10^6\ M^{-1}$, which is one order of magnitude smaller than that of **64**. Therefore, the π–electronic conjugation along the backbone plays an important role in the electron transfer to MV^{2+}.

Fluorescence–quenching profiles are highly dependent on the generation number and the surface of the dendrimer framework. For example, the lowest–generation **62** displays a low fluorescence–quenching activity, with a maximum quenching degree of only one–seventh that of **64**. In contrast, positively charged compound **65** does not exhibit fluorescence quenching, even at high $[MV^{2+}]$, indicating that MV^{2+} cannot be trapped on the dendrimer surface due to electrostatic repulsion. On the other hand, **67**, a nonionic derivative of **64** bearing tetraethylene glycol chains on the dendrimer surface, does not show quenching at all, even in the presence of large excess MV^{2+}. Therefore, several structural factors are cooperative to achieve the efficient photoinduced electron transfer in the above system. The inherent photoactivity of the poly(phenyleneethynylene) backbone, because of a long–range π–conjugation, is essential for the high photosensitivity of the system. Of equal importance is that, the large dendrimeric shell helps isolate the conjugated backbone and maintain the inherently high photoactivity even in water. Finally, the negative charges on the dendrimer surface are also essential for the acceptor to be trapped within an electron–transfer distance from the conjugated backbone.

Continuous exposure of a mixture of the Tris–HCl buffer of **64** and MV^{2+}, in the presence of triethanolamine (TEOA) as a sacrificial donor to a 150–W Xenon arc light results in catalytic photoreduction of MV^{2+} to $MV^{+\bullet}$, with an overall quantum efficiency (Φ = number of $MV^{+\bullet}$/number of photons absorbed) of 29%. In contrast, systems with one–generation smaller **63** and lowest–generation **62** show lower catalytic photoreduction activity, whereas positively charged **65** does not respond to light irradiation at all. Of much interest, π–electronic conjugation of the backbone also significantly affects the photoreduction. For example, In contrast to the heptamer **66** that shows relatively high efficiency (30%), both short–chain **68** and *meta*–linked **69** exhibit only low efficiency of 3 and 5%, respectively. In the terms of efficiency, **64** is also supreme to representative sensitizers, such

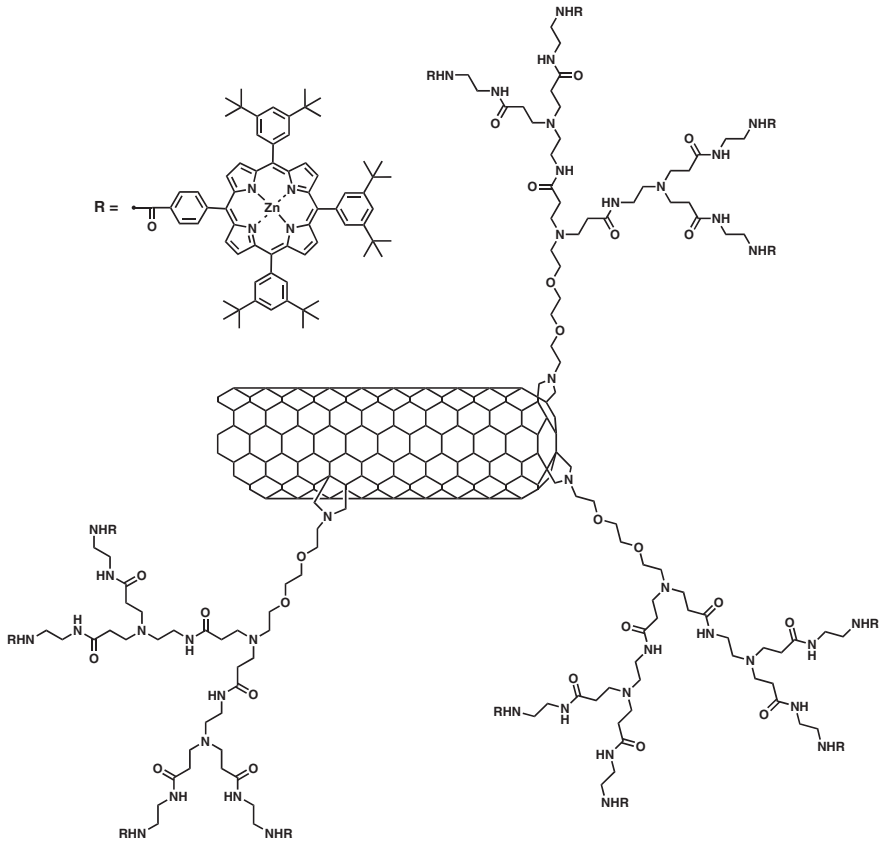

61

as $Ru(bpy)_3Cl_2$, 10–methyl–acridine orange, and zinc tetrakis(1–methylpyridinium–4–yl)porphyrin, which show Φ values of only 1, 3 and 6%, respectively. Based on these results, the above photoreduction system has been further coupled with PVA–Pt colloidal as a catalyst for hydrogen evolution. The **64**/MV^{2+}/TEOA/PVA–Pt system shows a steady generation of hydrogen without a decrease in activity during 5–h irradiation and is tolerant to photo–bleaching. The overall quantum efficiency for hydrogen evolution (number of H_2 molecules generated/number of photons absorbed) has been evaluated as 13%, which is more than one order of magnitude higher than those of previously reported systems.

The built–in dendrimeric core–shell strategy reveals the great potential of conjugated polymers as highly efficient photosensitizers for hydrogen evolution from water. Three–dimensional wrapping with a surface–charged large dendrimeric shell allows the suppress of self–quenching of the photoexcited conjugated backbone, while MV^{2+} is trapped on the negatively charged dendrimer surface to form a spatially separated donor–acceptor supramolecular complex. Together with this unique donor–acceptor geometry, hole migration along the conjugated backbone might lower the relative rate of charge recombination. This is also suppressed by a rapid exchange of $MV^{+\bullet}$ with MV^{2+} in the bulk solution, due to the lower affinity of the former towards the negatively charged dendrimer surface. Consequently, the energy of visible photons harvested by the conjugated wire chain flows steadily into MV^{2+} and is stored as $MV^{+\bullet}$, which triggers hydrogen evolution from water. Dendritic architectures are unique in that they possess a unique mechanical stability unlike micellar aggregates, whilst maintaining appropriate conformational change dynamics. These properties cast a sharp contrast to other nanoscopic architectures, such as inorganic multilayers and zeolite pores, which have previously been investigated as intervening media for electron–transfer reactions.

Other Dendritic PET Systems

As mentioned above, fullerene is an attractive electron acceptor to afford long–lived charge–separation states because of small reorganization energy. Other than porphyrin derivatives as electron–donating components, a variety of dendritic systems for photoinduced electron transfer reaction have been reported using amine, cytochrome *c*, and phenanthlorine copper(I) complex as electron donors.[74–79] Utilization of the dendrimer framework to encapsulate acceptor moieties *c.f.* viologen[80,81] and norbornadiene,[82] or donor units such as ruthenium bipyridine complex[83]

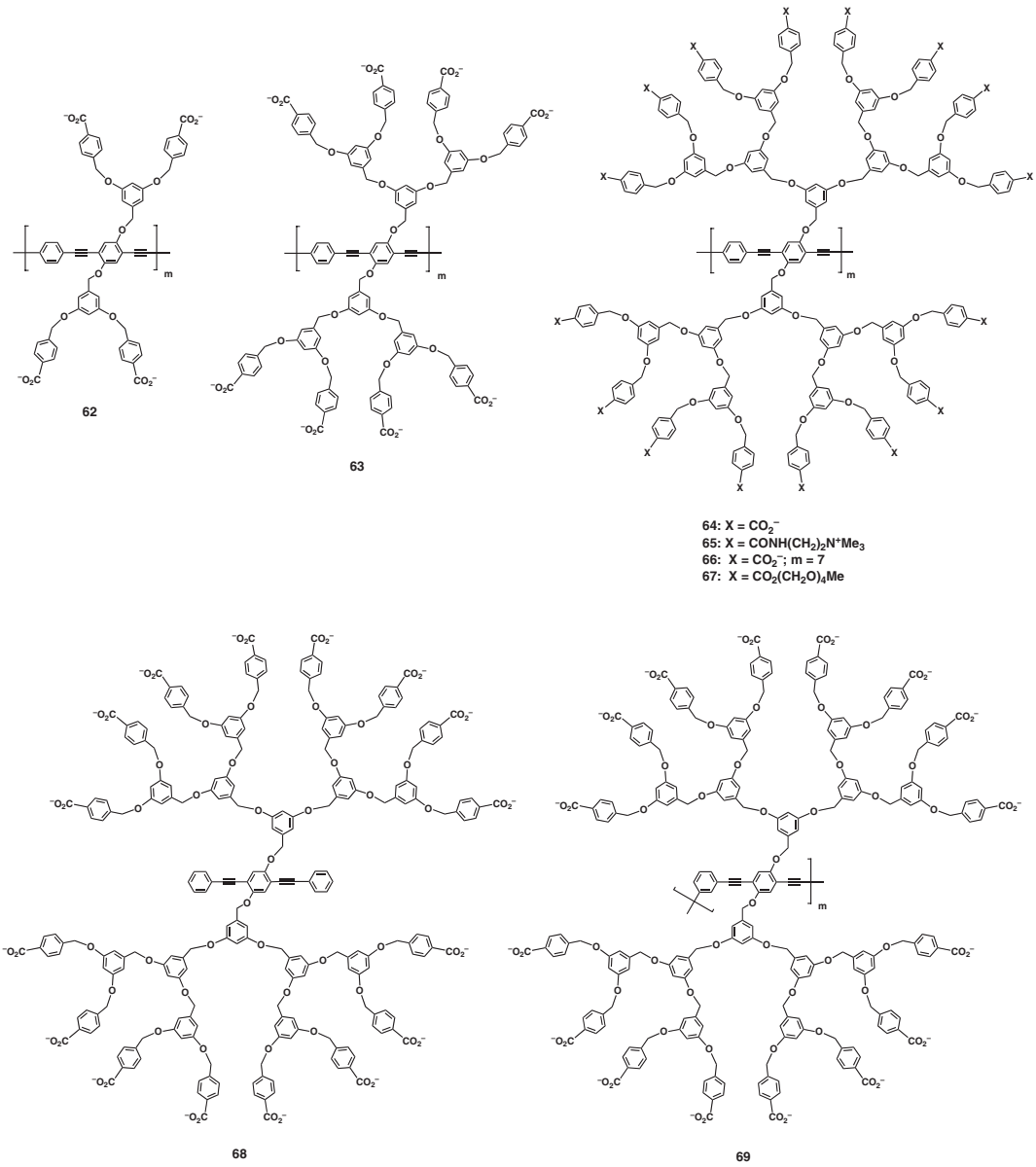

and anthracene[84] have also been reported for the construction of electron transfer systems. A further extension of using dendrimers for triggering photoinduced electron transfer is to employ photoactive units as the building blocks in the framework. In this sense, poly(phenyl acetylene) dendrimer is unique since the whole dendrimer framework can serve as electron–donating or electron–accepting components, highly depending on the external electron–active molecules utilized.[85] In relation to this, recently, a series of poly(viologen) dendrimers with different numbers of viologen units have been synthesized by Marchioni and coworkers to investigate the stepwise photoreduction of viologen arrays in the bulky dendrimer framework.[86]

A well–defined three–dimensional structure along with a precise location of functional groups in its framework makes dendritic macromolecule a promising motif for the investigation of photoinduced electron transfer event at the single molecular level. Recently, De Schryver and coworkers have explored this possibility by using rigid polyaryl dendrimers **70** and **71** with peryleneimide core as electron acceptor and arylamine units on the surface as electron donor, upon embedded in a polystyrene matrix.[87] In general, photoinduced electron transfer process is hardly to be monitored with single–molecule spectroscopy, because the fluorescence is usually quenched and no signals can be detected. However, the charge–separation states of **70** and **71** decay to form again locally excited state through a reverse electron transfer process. Therefore, the delayed fluorescence with a high quantum yield enables the monitor of photoinduced electron transfer event with single–molecule spectroscopy. Dynamic fluctuations of the fluorescence decay times have been observed for **70**. A

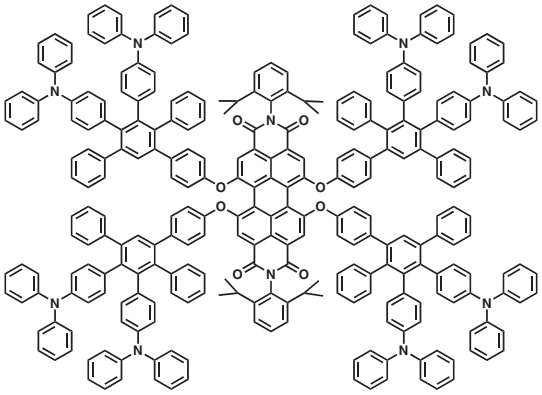

70

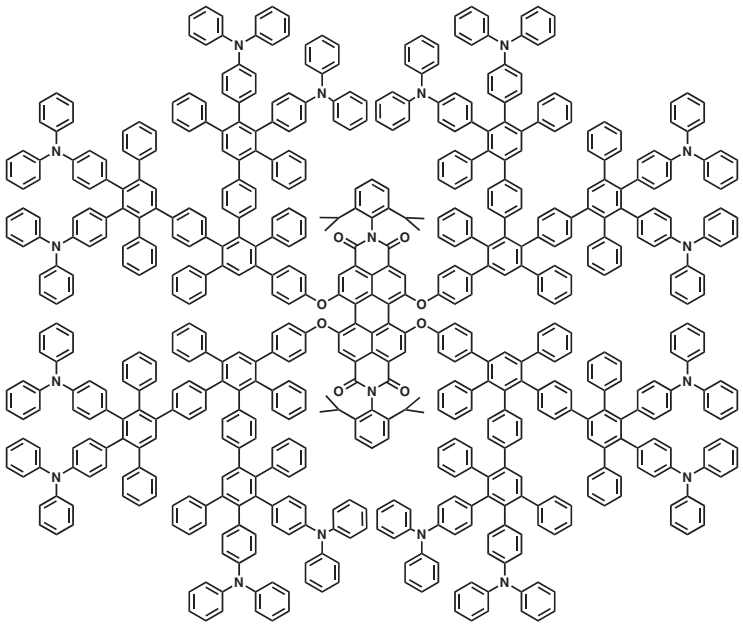

71

detailed study shows that the conformational changes of the dendrimers (**70** and **71**) and reorientation of the matrix polystyrene chains induce the fluctuations of the fluorescence decay times. The torsional motion of the adjacent phenyl rings next to the donor in the dendrimer is attributable to the small fluctuations in decay times, whereas polystyrene motion causes much dynamic conformational change of the dendrimer and thereby leads to the large fluctuations.[87e]

Dendrimers for Photoinduced Hole Transfer

As described above, the dendrimer framework serves as light–harvesting antenna and mediates photoinduced electron transfer. In relation to these functions, to explore dendrimer for hole transfer is a subject of importance, due to its high possibility to develop hole–transporting materials for organic light–emitting diodes (OLEDs). Photoinduced hole transfer within the dendrimer framework has been reported by Hara, Majima, and coworkers in a poly(benzyl ether) dendrimer **72** with stilbene focal core.[88] Two–photon excitation of the dendrimer framework at 266 nm generates a hole in the dendrimer framework. The hole thus produced can further transfer to the focal stilbene core to result in the formation of stilbene cationic radical. As the generation number of the dendrimer framework increases, the lifetime of stilbene cationic radical increases, as a result of site isolation. Although the quantum yield of two–photon ionization is low as 6.9%, the hole transfer efficiency form the dendrimer framework to the focal stilbene core is quantitative. In a three–component system using biphenyl (BP) as a hole transporter, 9,10–dicyanoanthracene (DCAN) as a photosensitizer, and **72** as a hole trap, the same group have reported that photoexcitation of DCAN at 355 nm results in a consecutive electron and hole transfer, to afford stilbene cationic radical and DCAN anionic radical. As the generation

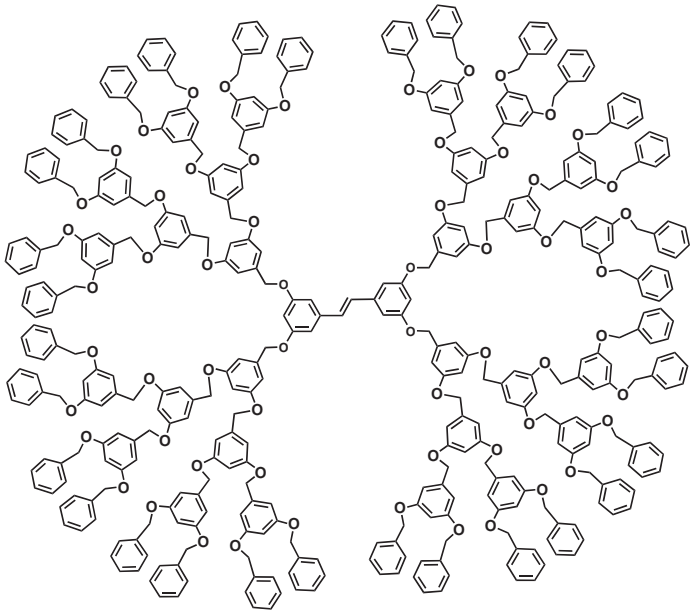

72

number increases from 1 to 4, the rate constant of intermolecular hole transfer from BP cationic radical to dendrimers remains unchanged (about 2×10^9 $M^{-1}\,s^{-1}$), but that of intramolecular hole transfer from exterior surface to the focal stilbene unit decreases from 4.2×10^6 to $1.6 \times 10^6\,s^{-1}$. The large dendrimer framework because of its steric hindrance, not only inhibits the direct hole–transfer from BP cationic radical to stilbene core but retards charge recombination between stilbene cationic radical and DCAN anionic radical as well.

Besides the above photo–generated hole transportation event in the dendrimer framework, electrically triggered hole transfer have also been investigated. Moore and coworkers have reported that an anthracene–cored poly(phenylene acetylene) dendrimer with triaryl amine units on the surface, can transport hole in OLEDs.[89] More recently, Yamamoto and coworkers have reported that poly(phenylazomethine) dendrimers upon complexation with Sn^{2+} show an activity in hole transport.[90]

DENDRITIC ARCHITECTURES FOR SPIN–FUNCTIONAL NANOMATERIALS

As described above, dendritic macromolecules are versatile in controlling electron charge to perform vectorial excitation energy transduction and efficient photoinduced electron transfer. On the other hand, to control electron spin with dendrimers has attracted much attention in recent years, with an even increasing interest due to their high probability for regulating spin–spin interactions. In contrast to traditional inorganic crystalline frameworks, dendrimers are unique in that they allow for designable 'engineering' of the spin–active components and the materials thus obtained can be easily processed. Therefore, by integrating suitable organic groups and/or segments, *c.f.* those responsive to external stimuli, one may have the chance to create novel spin–active soft materials.

Dendritic Organic Radicals

Organic radical compounds have been a central concern in relation to the development of magnetic soft materials with a recent focus on π–conjugated polymers, because of their possibility to achieve strong exchange interactions between spin sites through π–conjugation network. From a viewpoint of the molecular design, a system with a high density of cross links and alternating connectivity of radical sites is a structural prerequisite for achieving large values of spin–quantum number S.[91] Conjugated dendrimers have a high potential to fulfill these requirements and are promising motif to mediate spin–spin interactions, due to the possibility for 'tailor–made' placement of spin sites in the three–dimensional framework.

Veciana and coworkers have reported a dendritic polyradicals **73** with four radical sites based on poly(triphenyl methylene) dendrimer upon treatment with tetrabutyl ammonium hydroxide followed by oxidation with *p*–chloranil.[92] EPR measurement shows that **73** displays a profile due to the forbidden transition with $\Delta m_S = \pm 2$, but without any signs from transitions with $\Delta m_S = \pm 3$ and $\Delta m_S = \pm 4$. Magnetic–field dependency of the susceptibility indicates that the dendritic polyradicals **73** is mainly at a triplet state with an S value of 1. The fact that magnetic ground

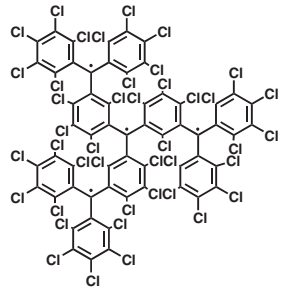

73

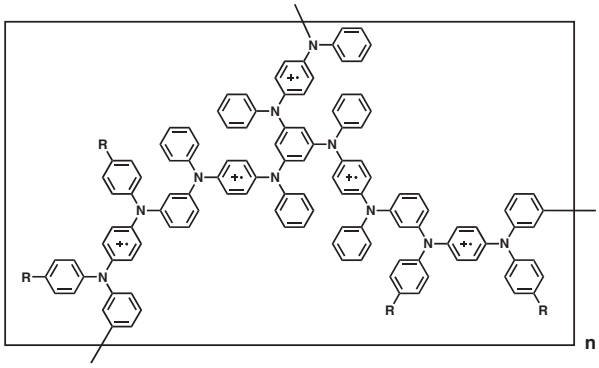

75

state of **73** is triplet other than quintet is likely due to the non–planarity of sp^2–central carbon induced by distortion of the neighboring large aromatic rings. The bulky dendrimer framework enhances the stability of high–spin species but simultaneously results in undesired spatial congestions, which may block ferromagenetic coupling between the spin sites.

Müllen and co–workers have synthesized polyphenylene dendrimers bearing eight trityl–radicals or trityl–anionic radicals in the frameworks.[93] In comparison with simple trityl–radical reference, dendritic trityl–radicals **74** exhibits a 70 nm red–shifted absorption band, suggesting an efficient delocalization of spin density over the dendrimer framework. The ground state of this dendritic trityl–radicals is $S = 1/2$, suggesting no ferromagnetic interactions take place between radical sites. On the other hand, the dendritic trityl–anionic radicals show a ground state with an S value of 1, derived from biradicals that are bridged by K^+ (introduced at the reduction step).

A dendrimer–like aromatic poly(aminium cationic radicals) **75** has been synthesized by Nishide and coworkers. **75** forms a 2–D polyradicals network with an S value of 8.4 at 5 K.[94] This high–spin ground state indicates a ferromagnetic coupling between eight or nine unpaired electrons at low temperature in the dendrimer–like poly(aminium cationic radicals).

TTF is an attractive motif to build up molecular conductors due to the formation of cationic radical in the presence of magnetic counter ions. Up to date,

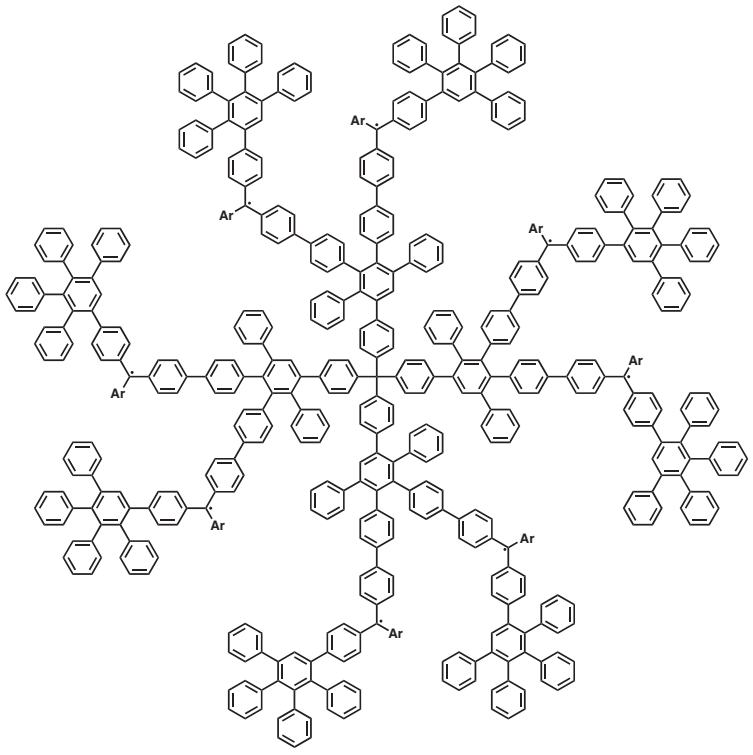

74

Ar = 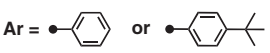 or

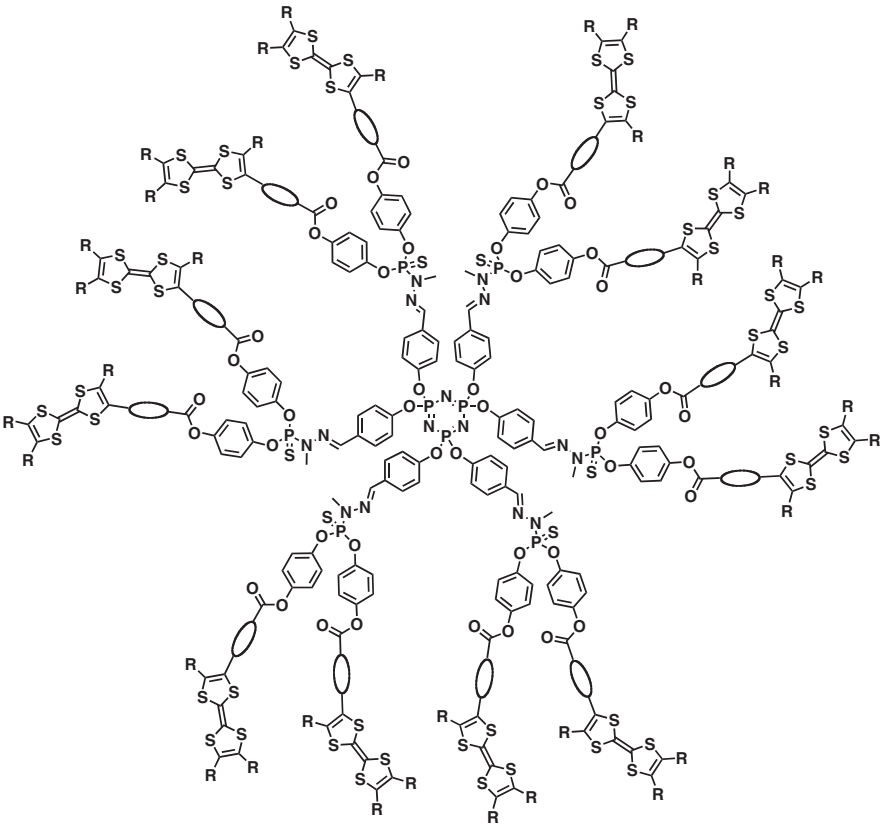

76

a variety of dendrimers containing TTF building blocks have been synthesized with an aim to achieve conductive and/or magnetic active materials.[95] Bryce and coworkers have synthesized a family of multi–TTF dendrimers.[96] Electrochemical oxidation of the multi–TTF dendrimers affords polycationic radical species. On the other hand, controlled chemical oxidation of a multi–TTF dendrimer **76** with $PhI(OAc)_2$ in the presence of CF_3SO_3H gives mixed–valence cationic radical salts, which show electric conductivity.[97] The conductivity is originated from electron transfer between partially oxidized dendrimers as well as intermolecular charge transfer.

Nitroxide radicals, owing to their broad applications as initiator, spin tag, and magnetic contrast agent, have attracted great attention in recent years.[98] Dendritic macromolecules containing nitroxide radicals have been synthesized mainly based on polyamine framework. Tomalia and coworkers immobilized TEMPO moiety to the exterior surface of polyamine dendrimer as a spin probe to gain structural information and to investigate interactions between dendrimers with mesoporous surface, vesicles, and liposomes.[99,100] Poly(propylene imine) dendrimers bearing multi–nitroxyl groups on the surface display strong exchange interaction between radical sites.[101] Upon anchoring on the poly(amide amine) dendrimer surface, Brechbiel and coworkers have reported that the TEMPO units are robust for EPR imaging to retain spin activity for a much longer period even in an aqueous solution.[102] In relation to this, Francese and coworkers have reported a water–soluble poly(amide amine) dendrimer with nitroxyl nitroxide radicals on the surface as a contrast agent for MRI.[103]

Spin–Transition Soft Materials Based on Dendritic Coordination Polymers

Metal complexes with d^4–d^7 first–row transition metal ions in octahedral environment exhibit a spin crossover (SCO) between low–spin (LS) and high–spin (HS) states under certain conditions. Such a bistability phenomenon has attracted intense attentions not only from the basic scientific viewpoint but also for its potential applications in molecular electronics. By employing chemical approaches such as crystal engineering, much effort has been made for the preparation of SCO crystalline solids, which suffer from the low processability.[104] Hence, it is yet a challenging subject to fabricate SCO soft materials that not only have tunable spin states by external stimuli but also have improved processability.[105–107]

Fujigaya and coworkers have reported SCO phe-

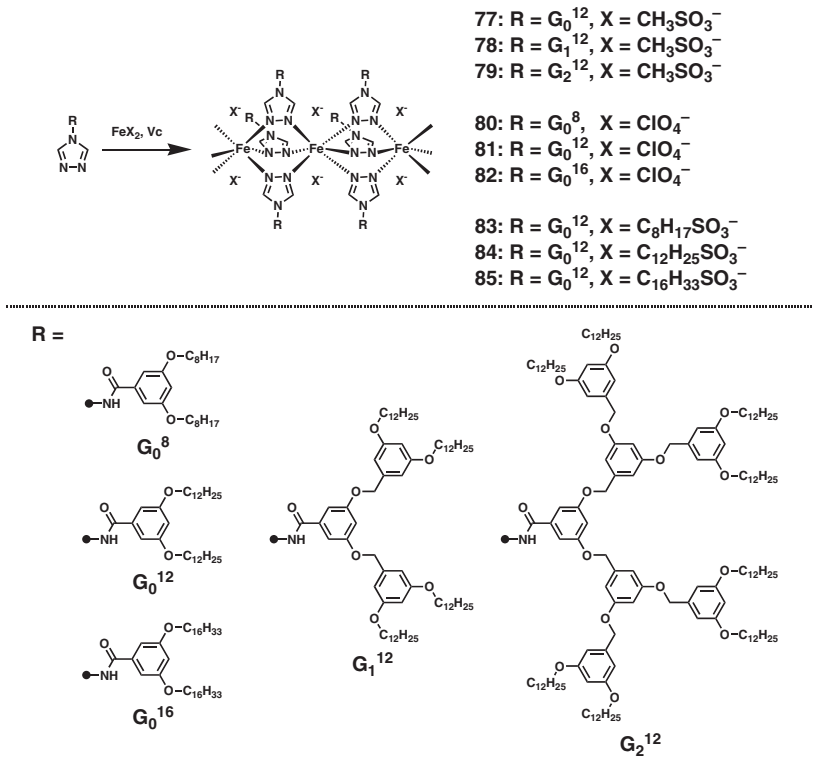

nomenon of dendritic Fe(II) triazole complexes **77**–**79** self–assembled from Fe(II) ions and dendritic triazole ligands with poly(benzyl ether) dendrons.[108] These complexes are colored violet at room temperature due to a *d*–*d* electronic transition of the LS Fe(II) species, and decoloration occurs upon heating to give off–white solids, as a result of spin transition to the HS state. Such a thermally induced spin transition is reversible and can be repeated for many times without any deterioration. Of interest, the spin transition is highly dependent on the generation number. SQUID measurement of **78** shows a complete spin transition in a temperature range of only 10 K, which is in good agreement with an abrupt coloration–decoloration response to the temperature change. In contrast, **77** and **79** require a much broader temperature range of 30 and 50 K, respectively. Besides, the spin–transition temperature decreases from 335 to 315 to 300 K when the generation number increases from 0 to 1 to 2.

DSC measurement shows that the ΔH and ΔS values for the spin transition of **77** are 15.7 kJ mol^{-1} and 46.7 J mol^{-1} K^{-1}, respectively, which are typical of those reported for spin transition of Fe(II)–triazole complexes.[109] Contrastingly, **78** exhibits much higher ΔH and ΔS values of 73.1 kJ mol^{-1} and 230.0 J mol^{-1} K^{-1}, respectively. In regard to the abrupt spin transition event together with the extraordinary high ΔH and ΔS values, the Fe(II) sites in self–assembled **78** are strongly correlated with one another and highly cooperate in the spin transition. In relation to this feature, **78** shows the most distinct X–ray diffraction (XRD) pattern among the series, which is indicative of a 2D hexagonal ordering with a *d*–spacing of 37.4 Å. Considering the Fe–Fe distance of 3.7 Å as evaluated by EXAFS, the unit cell has been calculated as 43.2 Å in diameter and 3.7 Å in height (V = 5.42 nm^3, W = 5.79 × 10^{-21} g). Since the density of the material, measured using a gradient density column, is 1.07 g cm^{-3}, the unit cell can accommodate 2.8 dendron subunits. This number is very close to the requisite stoichiometry of 3:1 for complexation between triazole and Fe(II). Thus, the dendritic wedges in **78** are densely packed around the oligomeric Fe(II)–triazole backbone and perfectly fit the surrounding space. In comparison to **78**, the unit cells of **77** and **79** are estimated to accommodate 4.1 and 1.6 units of dendron subunits, respectively, indicating that the dendritic wedge of **77** is not large enough to fill the unit cell, while the unit cell of **79** is not large enough to satisfy the ideal 3:1 complexation. From these results, it is most likely that self–assembled **77** and **79** are structurally defective and frustrative, so that the Fe(II) sites are hardly cooperative with one another for the spin transition. This study shows that dendrimers are useful components for design "cooperativity," which can enhance or amplify certain functions in self–organized states.

Spin–Transition Soft Materials Switchable with Phase Transitions

By appending the triazole unit with long alkyl chains of different lengths, *i.e.* C8, C12, and C16,

Fujigaya and coworkers have synthesized dendrimers **80**–**82** in which each Fe(II) is bridged by three bidentate triazole ligands to afford one–dimensional rod.[110] Of interest, the length of the alkyl chains strongly affects their SCO profiles. Compound **82** with the longest alkyl chains displays the spin transition at ~310 K with a hysteresis width of 5 K. Compound **81** exhibits a spin–crossover profile similar to that of **82**, whereas **80** with the shortest alkyl chains hardly shows a clear spin transition.

XRD pattern of **82** shows a *d* spacing of 36.5 Å, suggesting an interdigitation of the long alkyl chains to give parallel–aligned Fe(II)–triazole backbones, whose center–to–center separation is estimated to be 36 Å. **81** shows a similar XRD pattern but with a smaller *d* spacing of 30.2 Å. Thus, the Fe(II) centers are fastened to one another not only by ligation with the bidentate triazole ligands but also through interdigitation with the long alkyl chains.

Variable–temperature IR spectroscopy of **82** shows that the alkyl chains in LS state of **82** are crystallized with a stretched conformation, whereas those in HS state adopt a shrunk conformation. DSC measurements of **81** and **82** reveal that both show single endothermic and exothermic peaks, the transition temperatures of which are consistent with their spin–transition temperatures. Therefore, the phase transition of the alkyl chains triggers the SCO of **81** and **82**. At low temperatures, the crystalline alkyl chains, upon interdigitation, lock the Fe–N bond distance of the LS Fe(II) complexes. On heating, this lock is released by melting of the alkyl chains, thereby permitting the elongation of the Fe–N bond that is necessary for spin transition to the HS state. This supramolecular self–assembly approach allows mesoscopic cooperativity among the magnetic species through interdigitation of the alkyl chains, and thereby enables a 'lock–and–release' feature of the spin state.

Of interest, compound **83**–**85** having alkyl sulfonate as counter ion forms a purple–colored transparent physical gel in paraffins even at a low concentration such as 0.6 wt %.[111] Upon heating to 80 °C, the purple gel collapsed to give a pale yellow clear solution. Variable–temperature absorption spectroscopy on heating from 15 to 80 °C shows the appearance of a broad band centered at 850 nm, due to a $^5T_{2g}$–^5E_g *d*–*d* transition of the HS state, at the expense of the LS absorption band at 537 nm. On cooling to 15 °C, the hot solution immediately turns to a purple–colored transparent gel and recovers the LS absorption band at 537 nm. Such a thermal–induced discoloration–coloration cycle can be repeated without any sign of deterioration.

Polarized optical microscopy shows that self–assembly of **84** plays a major role in spin transition. A characteristic texture due to a liquid crystalline mesophase exists at 25 °C. Upon heating to induce the gel–to–sol phase transition, the liquid crystalline texture disappears completely at 62 °C. Rheological study at 25 °C shows that the system consists of a long–range alignment of rod–like **84**. Temperature–dependent rheological properties of **84** show that sol–gel transition occurs at a temperature same as that for the spin transition, indicating that the spin–transition and phase–transition events are perfectly synchronous to each other.

The spin–transition events of the gels are much quicker than those in solution. Both the transitions from the LS to HS and from HS to LS states are established only within a very short period of time (< 2 min). In sharp contrast, a *m*-xylene solution of **84** (0.6 wt %) shows an extremely slow recovery (> 300 min) of the LS state on rapid cooling from 50 to 20 °C. VT FT–IR measurement shows that a hydrogen–bonding network plays an important role in stabilization of the LS state. Therefore, mixing the gel of **84** with 1-octanol, which is a scavenger of the hydrogen bonding, results in spin transition and gel–to–sol phase transition simultaneously. In fact, on addition of different amounts of 1–octanol to the gel, the spin–transition temperature can be changed over a wide range from 65 to 20 °C.

The spin–crossover gels are characterized by their narrower temperature range for the spin transition than the solid samples, synchronous to the sol–gel phase transition, and their quick response to temperature changes both on heating and cooling. Since gels are generally more sensitive than solids to external perturbations, the spin–crossover gels may have a large potential in, *e.g.*, sensory applications.

SUMMARY

This article deals with two aspects of molecular functionality based on dendritic architectures; one is related to photoinduced energy and electron transfer and the other concerns spin state regulation. One may notice that cooperativity is one of the most unique characteristics of a dendritic macromolecule, which enables the enhancement of certain functions and/or creation of new phenomena. The role of the dendrimer framework is multiple and can be synthetically designable. In this sense, the well–defined and nano–sized dendritic macromolecules will continue to grow to be a central player in the materials science and serve as an interesting and fascinating motif in nanoscience, nanotechnology, and other interdisciplinary fields.

Acknowledgment. This work was partially supported by JSPS Asian CORE Program on Frontiers of Materials, Photo, and Theoretical Molecular Sciences.

REFERENCES

1. E. Buhleier, W. Wehner, and F. Vögtle, *Synthesis*, 155 (1978).
2. a) D. A. Tomalia, H. Baker, J. Dewald, M. Hall, G. Kallos, S. Martin, J. Roeck, J. Ryder, and P. Smith, *Polym. J.*, **17**, 117 (1985).
   b) D. Tomalia, *Adv. Mater.*, **6**, 529 (1994).
3. a) C. J. Hawker and J. M. J Fréchet, *J. Chem. Soc., Chem. Commun.*, **14**, 1010 (1990).
   b) C. J. Hawker and J. M. J. Fréchet, *J. Am. Chem. Soc.*, **112**, 7638 (1990).
   c) C. J. Hawker and J. M. J. Fréchet, *Macromolecules*, **23**, 4726 (1990).
4. "Dendrimers and other dendritic polymers," J. M. J. Fréchet and D. Tomalia, Ed., Wiley-VCH, Weinheim, 2001.
5. T. Aida and D.-L. Jiang, in "The porphyrin handbook Vol. 3. Inorganic, organometallic, and coordination chemistry," K. M. Kadish, K. M. Smith, and R. Guilard, Ed., Academic Press, New York, 2000, p 369.
6. G. McDermott, S. M. Prince, A. A. Freer, A. M. Hawthornthwaite-Lawless, M. Z. Papiz, R. J. Cogdell, and N. W. Isaacs, *Nature*, **374**, 517 (1995).
7. W. Kühlbrandt, *Nature*, **374**, 497 (1995).
8. A. M. van Oijen, M. Ketelaars, J. Köhler, T. J. Aartsma, and J. Schimidt, *Science*, **285**, 400 (1999).
9. D.-L. Jiang and T. Aida, *Prog. Polym. Sci.*, **30**, 403 (2005).
10. D.-L. Jiang and T. Aida, *J. Am. Chem. Soc.*, **120**, 10895 (1998).
11. H. Sato, D.-L. Jiang, and T. Aida, *J. Am. Chem. Soc.*, **121**, 10658 (1999).
12. S. Masuo, H. Yoshikawa, T. Asahi, H. Masuhara, D.-L. Jiang, and T. Aida, *J. Phys. Chem. B*, **105**, 2885 (2001).
13. S. Masuo, H. Yoshikawa, T. Asahi, H. Masuhara, D.-L. Jiang, and T. Aida, *J. Phys. Chem. B*, **106**, 905 (2002).
14. S. Masuo, H. Yoshikawa, T. Asahi, H. Masuhara, D.-L. Jiang, and T. Aida, *J. Phys. Chem. B*, **107**, 2471 (2003).
15. W.-S. Li, D.-L. Jiang, and T. Aida, *Angew. Chem. Int. Ed.*, **43**, 2943 (2004).
16. N. Sabbatini, M. Guardigli, and J.-M. Lehn, *Coord. Chem. Rev.*, **123**, 201 (1993).
17. M. Kawa and J. M. J. Fréchet, *Chem. Mater.*, **10**, 286 (1998).
18. M. Kawa and J. M. J. Fréchet, *Thin Film Solids*, **331**, 259 (1998).
19. M. Kawa and T. Takahagi, *Chem. Mater.*, **16**, 2282 (2004).
20. N. S. Baek, Y. H. Kim, S.-G. Roh, B. K. Kwak, and H. K. Kim, *Adv. Funct. Mater.*, **16**, 1873 (2006).
21. F. Vögtle, M. Gorka, V. Vicinelli, P. Ceroni, M. Maestri, and V. Balzani, *ChemPhysChem*, **12**, 769 (2001).
22. V. Vicinelli, P. Ceroni, M. Maestri, V. Balzani, M. Gorka, and F. Vögtle, *J. Am. Chem. Soc.*, **124**, 6461 (2002).
23. S. L. Gilat, A. Adronov, and J. M. J. Fréchet, *Angew. Chem. Int. Ed.*, **38**, 1422 (1999).
24. A. Adronov, S. L. Gilat, J. M. J. Fréchet, K. Ohta, F. V. R. Neuwahl, and G. R. Fleming, *J. Am. Chem. Soc.*, **122**, 1175 (2000).
25. a) T. Z. Förster, *Naturforsach Teil. A.*, **4**, 319 (1949).
    b) B. W. Van der Meer, G. Coker III, and S. Y. Simon Chen, "Resonance Energy Transfer, Theory and Data," VCH: Weinheim, 1994.
26. A. Adronov, P. R. L. Malenfant, and J. M. J. Fréchet, *Chem. Mater.*, **12**, 1463 (2000).
27. J. M. Serin, D. W. Brousmiche, and J. M. J. Fréchet, *Chem. Commun.*, 2605 (2002).
28. M. Wind, U.-M. Wiesler, K. Saalwächter, K. Müllen, and H. W. Spiess, *Adv. Mater.*, **13**, 752 (2001).
29. T. Weil, E. Reuther, and K. Müllen, *Angew. Chem. Int. Ed.*, **41**, 1900 (2002).
30. L. A. J. Chrisstoffels, A. Adronov, and J. M. J. Fréchet, *Angew. Chem. Int. Ed.*, **39**, 2163 (2000).
31. J. Seth, V. Palaniappan, R. W. Wagner, T. E. Johnson, J. S. Lindsey, and D. F. Bocian, *J. Am. Chem. Soc.*, **118**, 11194 (1996).
32. M.-S. Choi, T. Yamazaki, I. Yamazaki, and T. Aida, *Angew. Chem. Int. Ed.*, **43**, 150 (2004).
33. D. Kim and A. Osuka, *Acc. Chem. Res.*, **37**, 735 (2004).
34. M.-S. Choi, T. Aida, T. Yamazaki, and I. Yamazaki, *Angew. Chem. Int. Ed.*, **40**, 3194 (2001).
35. M.-S. Choi, T. Aida, T. Yamazaki, and I. Yamazaki, *Chem. Eur. J.*, **8**, 2668 (2002).
36. S.-I. Kimata, D.-L. Jiang, and T. Aida, *J. Polym. Sci., Part A: Polym. Chem.*, **41**, 3524 (2003).
37. W.-S. Li, D.-L. Jiang, Y. Suna, and T. Aida, *J. Am. Chem. Soc.*, **127**, 7700 (2005).
38. S. Cho, W.-S. Li, M.-C. Yoon, T. K. Ahn, D.-L. Jiang, J. Kim, T. Aida, and D. Kim, *Chem. Eur. J.*, **12**, 7576 (2006).
39. C. C. Mak, D. Pomeranc, M. Montalti, L. Prodi, and J. K. M. Sanders, *Chem. Commun.*, 1083 (1999).
40. M. R. Benites, T. E. Johnson, S. Weghorn, L. Yu, P. D. Rao, J. R. Diers, S. I. Yang, C. Kirmaier, D. F. Bocian, D. Holten, and J. S. Lindsey, *J. Mater. Chem.*, **12**, 65 (2002).
41. M. R. Wasielewski, *J. Org. Chem.*, **71**, 5051 (2006).
42. T. Van der Boom, R. T. Hayes, Y. Zhao, P. J. Bushard, E. A. Weiss, and M. R. Wasielewski, *J. Am. Chem. Soc.*, **124**, 9582 (2002).
43. M. J. Ahrens, L. E. Sinks, B. Rybtchinski, W. Liu, B. A. Jones, J. M. Giaimo, A. V. Gusev, A. J. Goshe, D. M. Tiede, and M. R. Wasielewski, *J. Am. Chem. Soc.*, **126**, 8284 (2004).
44. X. Li, L. E. Sinks, B. Rybtchinski, and M. R. Wasielewski, *J. Am. Chem. Soc.*, **126**, 10810 (2004).
45. D.-L. Jiang and T. Aida, *Nature*, **388**, 454 (1997).
46. T. Aida, D.-L. Jiang, E. Yashima, and Y. Okamoto, *Thin Solid Films*, **331**, 254 (1998).
47. Y.-J. Mo, D.-L. Jiang, M. Uyemura, T. Aida, and T. Kitagawa, *J. Am. Chem. Soc.*, **127**, 10020 (2005).
48. W. L. Peticolas, *Ann. Phys. Leipzig*, **18**, 233 (1967).
49. W. M. McClain, *Acc. Chem. Res.*, **7**, 129 (1974).
50. R. R. Birge and B. M. Pierce, *J. Chem. Phys.*, **70**, 165 (1979).
51. M. Göppert-Mayer, *Ann. Phys.*, **9**, 273 (1931).
52. A. Adronov and J. M. J. Fréchet, *Chem. Mater.*, **12**, 2838 (2000).
53. D. W. Brousmiche, J. M. Serin, J. M. J. Fréchet, G. S. He, T.-C. Lin, S. J. Chung, and P. N. Prasad, *J. Am. Chem. Soc.*, **125**, 1448 (2003).

54. D. W. Brousmiche, J. M. Serin, J. M. J. Fréchet, G. S. He, T.-C. Lin, S. J. Chung, P. N. Prasad, R. Kannan, and L.-S. Tan, *J. Phys. Chem. B*, **108**, 8592 (2004).
55. R. Bonnett, *Chem. Soc. Rev.*, **24**, 19 (1995).
56. R. Bonnett and G. Martinez, *Tetrahedron*, **57**, 9513 (2001).
57. M. C. DeRosa and R. J. Crutchlley, *Coord. Chem. Rev.*, **233–234**, 351 (2003).
58. W. R. Dichtel, J. M. Serin, C. Edder, J. M. J. Fréchet, M. Matuszewski, L.-S. Tan, T. Y. Ohulchanskyy, and P. N. Prasad, *J. Am. Chem. Soc.*, **126**, 5380 (2004).
59. M. A. Oar, J. M. Serin, W. R. Dichtel, J. M. J. Fréchet, T. Y. Ohulchanskyy, and P. N. Prasad, *Chem. Mater.*, **17**, 2267 (2005).
60. S. A. Vinogradov, *Org. Lett.*, **7**, 1761 (2005).
61. R. P. Briñas, T. Troxler, R. M. Hochstrasser, and S. A. Vinogradov, *J. Am. Chem. Soc.*, **127**, 11851 (2005).
62. "Porphyrin Handbook," K. M. Kadish, K. M. Smith, and R. Guilard, Ed., Academic Press, New York, 1999.
63. R. Sadamoto, N. Tomioka, and T. Aida, *J. Am. Chem. Soc.*, **118**, 3978 (1996).
64. K. W. Pollack, J. W. Leon, J. M. J. Frechet, M. Maskus, and H. D. Abruna, *Chem. Mater.*, **10**, 30 (1998).
65. a) G. J. Capitosti, S. J. Cramer, C. S. Rajesh, and D. A. Modarelli, *Org. Lett.*, **3**, 1645 (2001).
b) C. S. Rajesh, G. J. Capitosti, S. J. Cramer, and D. A. Modarelli, *J. Phys. Chem. B*, **105**, 10175 (2001).
c) G. J. Capitosti, C. D. Guerrero, D. E. Binkley, C. S. Rajesh, and D. A. Modarelli, *J. Org. Chem.*, **68**, 247 (2003).
66. X. Camps, E. Dietel, A. Hirsch, S. Pyo, L. Echegoyen, S. Hackbarth, and B. Roder, *Chem. Eur. J.*, **5**, 2362 (1999).
67. M.-S. Choi, T. Aida, H. Luo, Y. Araki, and O. Ito, *Angew. Chem. Int. Ed.*, **42**, 4060 (2003).
68. R. Charvet, D.-L. Jiang, and T. Aida, *Chem. Commun.*, 2664 (2004).
69. W. S. Li, K. S. Kim, D.-L. Jiang, H. Tanaka, T. Kawai, J. H. Kwon, D. Kim, and T. Aida, *J. Am. Chem. Soc.*, **128**, 10527 (2006).
70. S. Campidelli, C. Sooambar, E. Lozano Diz, C. Ehli, D. M. Guldi, and M. Prato, *J. Am. Chem. Soc.*, **128**, 12544 (2006).
71. a) M. Sakamoto, A. Ueno, and H. Mihara, *Chem. Commun.*, 1741 (2000).
b) M. Sakamoto, A. Ueno, and H. Mihara, *Chem. Eur. J.*, **7**, 2449 (2001).
c) M. Sakamoto, T. Kamachi, I. Okura, A. Ueno, and H. Mihara, *Biopolymers*, **59**, 103 (2001).
72. S. Ogasawara, A. Ikeda, and J. Kikuchi, *Chem. Mater.*, **18**, 5982 (2006).
73. D.-L. Jiang, C.-K. Choi, K. Honda, W.-S. Li, T. Yuzawa, and T. Aida, *J. Am. Chem. Soc.*, **126**, 12084 (2004).
74. R. Kunieda, M. Fujitsuka, O. Ito, M. Ito, Y. Murata, and K. Komatsu, *J. Phys. Chem. B*, **106**, 7193 (2002).
75. Y. Araki, R. Kunieda, M. Fujitsuka, O. Ito, J. Motoyoshiya, H. Aoyama, and Y. Takaguchi, *C. R. Chimie*, **9**, 1014 (2006).
76. M. Braun, S. Atalik, D. M. Guldi, H. Lanig, M. Brettreich, S. Burghardt, M. Hatzimarinaki, E. Ravanlli, M. Prato, R. van Eldik, and A. Hirsch, *Chem. Eur. J.*, **9**, 3867 (2003).
77. N. Armaroli, C. Boudon, D. Felder, J. O. Gisselbrecht, M. Gross, G. Marconi, J. F. Nicoud, J. F. Nierengarten, and V. Vicinelli. *Angew. Chem. Int. Ed.*, **38**, 3730 (1999).
78. R. A. J. Janssen, J. F. G. A. Janssen, J. A. E. H. van Haare, and E. W. Meijer, *Adv. Mater.*, **6**, 494 (1996).
79. L. Dai, J. Lu, B. Matthews, and A. W. H. Mau, *J. Phys. Chem. B*, **102**, 4049 (1998).
80. M. Alvaro, B. Ferre, and H. Garcia, *Chem. Phys. Lett.*, **351**, 374 (2002).
81. T. H. Ghaddar, J. F. Wishart, D. W. Thompson, J. K. Whitesell, and M. A. Fox, *J. Am. Chem. Soc.*, **124**, 8285 (2002).
82. a) J. Chen, L. Zhang, S. Li, Y. Y. Li, J. Chen, G. Yang, and Y. Li, *J. Photochem. Photobiol. A. Chem.*, **185**, 67 (2007).
b) J. Chen, S. Li, L. Zhang, B. Liu, Y. Han, G. Yang, and Y. Li, *J. Am. Chem. Soc.*, **127**, 2165 (2005).
c) J. Chen, J. Chen, S. Li, L. Zhang, G. Yang, and Y. Li, *J. Phys. Chem. B*, **110**, 4663 (2006).
83. a) F. Vogtle, M. Plevoets, M. Nieger, G. C. Azzelini, A. Credi, L. De Cola, V. De Marchis, M. Ventuli, and V. Balzani, *J. Am. Chem. Soc.*, **121**, 6290 (1999).
b) A. Dirksen and L. De Cola, *C. R. Chimie*, **6**, 873 (2003).
84. S. V. Aathimanikandan, B. S. Sandanaraj, C. G. Agres, C. J. Bardeen, and S. Thayumanavan, *Org. Lett.*, **7**, 2809 (2005).
85. C. Devadoss, P. Bharathi, and J. S. Moore, *Macromolecules*, **31**, 8091 (1991).
86. F. Marshioni, M. Venturi, P. Ceroni, V. Balzani, M. Belohradsky, A. M. Elizarov, H. R. Tseng, and J. F. Stoddart, *Chem. Eur. J.*, **10**, 6361 (2004).
87. a) M. Lor, J. Thielemans, L. Viaene, M. Cotlet, J. Hofkens, T. Weil, C. Hampel, K. Müllen, J. W. Verhoeven, M. V. de Auweraer, and F. C. De Schryver, *J. Am. Chem. Soc.*, **124**, 9918 (2002).
b) M. Lor, S. Jorden, G. De Belder, G. Schweitzer, E. Fron, L. Viaene, M. Cotlet, T. Weil, K. Müllen, J. W. Verhoeven, M. Van der Auweraer, and F. C. De Schryver, *Photochem. Photobiol. Sci.*, **2**, 501 (2003).
c) R. Gronheid, A. Stefan, M. Cotlet, J. Hofkens, J. Qu, K. Müllen, M. V. der Auwraer, J. W. Verhoeven, and F. C. De Schryver, *Angew. Chem. Int. Ed.*, **42**, 4209 (2003).
d) M. Cotlet, S. Masuo, M. Lor, E. Fron, M. V. der Auweraer, K. Müllen, J. Hofkens, and F. C. De Schryver, *Angew. Chem. Int. Ed.*, **43**, 6116 (2004).
e) M. Cotlet, S. Masuo, G. Luo, J. Hofkens, M. V. der Auweraer, J. Verhoeven, K. Müllen, X. S. Xie, and F. C. De Schryver, *Proc. Natl. Acad. Sci. U.S.A.*, **101**, 14343 (2004).
88. a) M. Hara, S. Samori, X. Cai, S. Tojo, T. Arai, A. Momotake, J. Hayakawa, M. Uda, K. Kawai, M. Endo, M. Fujitsuka, and T. Majima, *J. Am. Chem. Soc.*, **126**, 14217 (2004).
b) M. Hara, S. Samori, X. Cai, S. Tojo, T. Arai, A. Momotake, J. Hayakawa, M. Uda, K. Kawai, M. Endo, M. Fujitsuka, and T. Majima, *J. Phys. Chem. B*, **109**, 973 (2005).
89. P. W. Wang, Y. J. Liu, C. Devadoss, P. Bharathi, and J. S. Moore, *Adv. Mater.*, **8**, 237 (1996).
90. N. Satoh, J. S. Cho, M. Higuchi, and K. Yamamoto, *J. Am. Chem. Soc.*, **125**, 8104 (2003).

91. A. Rajca, J. Wongsriratanakul, and S. Rajca, *Science*, **294**, 1503 (2001).
92. D. Ruiz-Molina, J. Vidal-Gancedo, N. Ventosa, J. Campo, F. Palacio, C. Rovira, and J. Veciana, *J. Phys. Chem. Solid*, **65**, 737 (2004).
93. S. Bernhardt, M. Baumgarten, M. Wagner, and K. Müllen, *J. Am. Chem. Soc.*, **127**, 12392 (2005).
94. T. Michinobu, J. Inui, and H. Nishide, *Org. Lett.* **5**, 2165 (2003).
95. J. L. Segura and N. Martín, *Angew. Chem. Int. Ed.*, **40**, 1372 (2001).
96. a) W. Devonport, M. R. Bryce, G. J. Marshallsay, A. J. Moore, and L. M. Goldenberg, *J. Mater. Chem.*, **8**, 1361 (1998).
b) C. A. Christensen, L. Goldenberg, M. R. Bryce, and J. Becher, *Chem. Commun.*, 509 (1998).
c) C. A. Christensen, M. R. Bryce, and J. Becher, *Synthesis*, **12**, 1695 (2000).
d) A. Beeby, M. R. Bryce, C. A. Christensen, G. Cooke, F. M. A. Duclairoir, and V. M. Rotello, *Chem. Commun.*, 2950 (2002).
97. A. Kanibolosky, S. Roquet, M. Cariou, P. Leriche, C.-O. Turrin, R. de Bettignies, A.-M. Caminade, J.-P. Majoral, V. Khodorkovsky, and A. Gorgues, *Org. Lett.*, **6**, 2109 (2004).
98. D. Abdallah, M. A. A. Ghani, M. F. Cunningham, P. M. Kazmaier, B. Keoshkerian, and E. Buncel, *Can. J. Chem.*, **82**, 1393 (2004).
99. M. F. Ottaviani, P. Matteini, M. Brustolon, N. J. Turro, S. Jokusch, and D. A. Tomalia, *J. Phys. Chem. B*, **102**, 6029 (1998).
100. M. F. Ottaviani, N. J. Turro, S. Jockush, and D. A. Tomalia, *J. Phys. Chem. B*, **107**, 2046 (2003).
101. A. W. Bosman, R. A. J. Janssen, and E. W. Meijer, *Macromolecules*, **30**, 3606 (1997).
102. A. T. Yordano, K. Yamada, M. C. Krishna, J. B. Mitchell, E. Woller, M. Cloninger, and M. W. Brechbiel, *Angew. Chem. Int. Ed.*, **40**, 2690 (2001).
103. G. Francese, F. A. Dunand, C. Loosli, A. E. Merbach, and S. Decurtins, *Magn. Reson. Chem.*, **41**, 81 (2003).
104. "Spin Crossover in Transition Metal Compounds I–III in Top Curr Chem," P. Gütlich and H. A. Goodwin, Ed., Weinheim: Springer-Verlag Berlin, Heidelberg, 2004.
105. O. Roubeau, A. Colin, V. Schmitt, and R. Clérac, *Angew. Chem. Int. Ed.*, **43**, 3283 (2004).
106. K. Kuroiwa, T. Shibata, S. Sasaki, M. Ohba, A. Takahara, T. Kunitake, and N. Kimizuka, *J. Polym. Sci., Part A: Polym. Chem.*, **44**, 5192 (2006).
107. M. Seredyuk, A. B. Gaspar, V. Ksenofontov, S. Reiman, Y. Galyametdinov, W. Haase, E. Rentschler, and P. Gütlich, *Chem. Mater.*, **18**, 2513 (2006).
108. T. Fujigaya, D.-L. Jiang, and T. Aida, *J. Am. Chem. Soc.*, **127**, 5484 (2005).
109. E. Konig, *Struct. Bonding*, **76**, 51 (1991).
110. T. Fujigaya, D.-L. Jiang, and T. Aida, *J. Am. Chem. Soc.*, **125**, 14690 (2003).
111. T. Fujigaya, D.-L. Jiang, and T. Aida, *Chem. Asian J.*, **2**, 106 (2007).

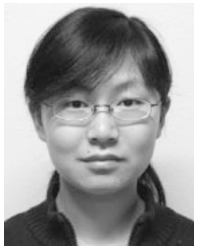

Zheng He received a B.S. degree from Peking University in 2000 and obtained a Ph.D degree in inorganic chemistry from the same university in 2005 under the supervision of Professor Chun–hua Yan. She started her postdoctoral work with Professor Donglin Jiang at Institute for Molecular Science, National Institutes of Natural Sciences from 2006. Her research interest is photo– and spin–functional dendritic macromolecules.

Tomoya Ishizuka received a B.S. degree in science from Kyoto University in 1999 and obtained a Ph.D. in chemistry from Graduate School of Science, Kyoto University in 2004 under the guidance by Professor Atsuhiro Osuka and Professor Hiroyuki Furuta (Kyushu University). Then, he became a postdoctoral fellow in University of Pennsylvania, working with Professor Michael J. Therien and received a JSPS Postdoctoral Fellowship for Research Abroad from April 2005. He joined as a research associate in the group of Professor Donglin Jiang at Institute for Molecular Science, National Institutes of Natural Sciences from February 2006 and became an assistant professor from April 2007 in the same group due to the change of the research faculty organization at IMS. His research interest is synthesis and new aspects of the physical properties of electronic and spin–functional materials.

Donglin Jiang received a B.S. degree in chemistry from Zhejiang University in 1989 and obtained a Ph.D. in polymer chemistry from The University of Tokyo in 1998 under the direction of Professor Takuzo Aida. He then became an academic carrier at The University of Tokyo and had been involved until 2000 in the development of functional polymers based on dendritic architecture. In 2000, he was appointed as a group leader of the JST ERATO project on "Nanospace." In 2005, he moved to Institute for Molecular Science, National Institutes of Natural Sciences as associate professor. His research interests include (1) synthesis and functions of metal polymers and (2) photo– and spin–functional dendritic macromolecules. In 2005, he was selected as a researcher of the JST PRESTO project on "Structure Control and Function." He received SPSJ Wiley Award 2006.